

Investigations of the Binding of Some Azido-, Isocyano-, and
Isothiocyanatochromium(III) and Azidocobalt(III) Complexes
with Heavy Metal Ions and Mercury Electrodes

Thesis by
Steven Neil Frank

In Partial Fulfillment of the Requirements
for the Degree of
Doctor of Philosophy

California Institute of Technology
Pasadena, California

1974

(Submitted July 11, 1973)

To my parents

Acknowledgments

I wish to express my sincerest gratitude to my research adviser, Fred C. Anson, for his advice and encouragement throughout these four years. He proved to me that patience is a virtue possessed by few men. I wish to acknowledge my thesis committee chairman, Joseph G. Gordon II, for his imperturbable good humor and advice.

Certain individuals deserve special mention for their contributions to my research and education. They are Donald J. Barclay and Hong Sup Lim for many hours of fruitful discussion and Roger Abel and Robert Rodgers for their computer expertise.

I also wish to acknowledge the friendship and aid I have received during my stay at Caltech from the following individuals (in alphabetical order), Drs. John Bercaw, Dusan Conrad, Predoctor Charles Cowman, Dr. Donald Ferrier, Predoctor Harry Finklea, Drs. Donald Glover, Jeffery Huntington, Eduardo Neves, Predoctor Bruce Parkinson, Drs. Alan Sears, V. S. Srinivasan, Michael Weaver and Chaim Yarnitzky.

I also wish to acknowledge Professors Harry B. Gray and Robert Stroud for reasons best left unsaid.

I give sincere thanks to Edi Bierce, the best secretary and thesis typist a graduate student ever had.

I wish to acknowledge Shell Companies Foundation, National Science Foundation and California Institute of Technology for financial support.

Abstracts

Part I. -- The reactions of $\text{Cr}(\text{OH}_2)_5\text{CN}^{2+}$, cis- $\text{Cr}(\text{OH}_2)_4(\text{CN})_2^+$, and fac- $\text{Cr}(\text{OH}_2)_3(\text{CN})_3$ with Hg^{2+} and Ag^+ to form binuclear and trinuclear adducts have been investigated. Equilibrium quotients

evaluated include:
$$\frac{[(\text{CrNC})_2\text{Hg}^{6+}]}{[\text{CrCN}^{2+}]^2[\text{Hg}^{2+}]} = 1.3 \pm 0.6 \times 10^{15};$$

$$\frac{[(\text{CrNC})_2\text{Ag}^{5+}]}{[\text{CrCN}^{2+}]^2[\text{Ag}^+]} = 5.6 \pm 5 \times 10^{10}; \quad \frac{[\text{CrNC}^{2+}]}{[\text{CrCN}^{2+}]} = 4.8 \pm 1 \times 10^{-3};$$

$$\frac{[\text{CrNCH}^{3+}]}{[\text{CrNC}^{2+}][\text{H}^+]} = 18 \pm 3.$$
 Electrochemical reduction of the heavy

metal adducts was utilized to generate a variety of the unstable isocyanochromium(III) isomers at mercury electrodes. No adsorptive binding of any of these complexes to the surface of the mercury electrodes could be detected. Possible reasons for the contrasting behavior displayed by the (nonadsorbing) isocyanochromium(III) and (strongly adsorbing) isothiocyanatochromium(III) complexes are examined.

Part II. -- The adsorption at mercury electrodes of a number of azido- and thiocyanatochromium(III) and azidocobalt(III) complexes has been measured with chronocoulometry. Apparent attractive interactions between adsorbed molecules were observed for the thiocyanato-complexes at some coverages. Several possible explanations are advanced to account for this behavior. A correlation between the amounts of adsorption and the ligand field stabilization energies (LFSE) of the complexes was observed. This correlation is discussed

in terms of an increase in the LFSE when the complexes bind with the electrode.

Table of Contents

	<u>Page</u>
Acknowledgments	iii
Abstracts	iv
Part I -- Binding of Some Cyano- and Isocyanochromium(III) Complexes with Hg(II), Ag(I) and Mercury Electrodes	1
Part II -- Adsorption of Azido- and Isothiocyanato- chromium(III) and Azidocobalt(III) Complexes on Mercury Electrodes	63
Propositions	129

Part I

Binding of Some Cyano- and Isocyanochromium(III) Complexes
with Mercury(II), Silver(I) and Mercury Electrodes

Part I is published in Inorganic Chemistry, 12, 2939 (1972).

The recent work of Espenson and co-workers^{1, 2} describing the reaction of $\text{Cr}(\text{OH}_2)_5\text{CN}^{2+}$ with Hg^{2+} to form a stable binuclear adduct, $(\text{H}_2\text{O})_5\text{CrNCHg}^{4+}$, attracted our interest because of the possibilities it suggested for substituting the positively charged surface of a mercury electrode for the Hg^{2+} ion to obtain the linkage isomerized chromium(III) complex adsorbed on the electrode surface where its electrochemical behavior could be observed.

The analogous system in which thiocyanate is the ligand by which mercury(II) is attached to chromium(III) has been studied in homogeneous solutions by Armor and Haim³ and at the surface of mercury electrodes.⁴ We were interested in testing whether the explanation proposed previously to account for the unusually strong bonding of the thiocyanato complexes to mercury electrodes⁴ would also apply to the corresponding isocyanochromium(III) complexes.

In a previous study⁵ the polarographic half-wave potential for $(\text{H}_2\text{O})_5\text{CrCN}^{2+}$ was given but an attempt to observe the reduction of the linkage isomer, $(\text{H}_2\text{O})_5\text{CrNC}^{2+}$, prepared via a homogeneous redox reaction, was not successful. We have found it possible to generate this isomer, as well as those obtainable from the di- and tricyano complexes, by electrochemical reduction of the heavy metal ions in the mercury(II) or silver(I) adducts that result when the chromium(III)-cyanide complexes are exposed to Hg^{2+} or Ag^+ . The electrochemical properties of the isocyano-linkage isomers are reported along with the composition and formation constants of the heavy metal adducts from which the isocyano complexes were generated.

Experimental Section

Materials. -- Except as noted, commercially available chemicals of reagent grade quality were used without additional purification. $[\text{Co}(\text{NH}_3)_5\text{CN}](\text{ClO}_4)_2$ was prepared according to Siebert.⁶

Commercial $\text{K}_3\text{Cr}(\text{CN})_6$ (Alpha Inorganics) proved to be rather impure and gave solutions with spectra that differed significantly from those of pure samples even after repeated recrystallization. However, solutions of CrCN^{2+} , $\text{Cr}(\text{CN})_2^+$, and $\text{Cr}(\text{CN})_3$ prepared by hydrolysis of the impure $\text{K}_3\text{Cr}(\text{CN})_6$ were indistinguishable from those obtained when spectroscopically pure $\text{K}_3\text{Cr}(\text{CN})_6$, prepared by slight modifications of published procedures,^{2, 7} was used.

Solutions of $(\text{H}_2\text{O})_5\text{CrCN}^{2+}$, cis- $(\text{H}_2\text{O})_4\text{Cr}(\text{CN})_2^+$, and fac- $(\text{H}_2\text{O})_3\text{Cr}(\text{CN})_3$ were prepared from $\text{Cr}(\text{CN})_6^{3-}$ by acid hydrolysis and separated by ion exchange.^{2, 8} Cr^{2+} prepared by electrolytic reduction of $\text{Cr}(\text{ClO}_4)_3$ was used to catalyze the hydrolysis reaction leading to CrCN^{2+} . The ion exchange resins employed were Bio-Rad AG 50W-X4, 100-200 mesh in the sodium form and Bio-Rad AG-1-X2, 200-400 mesh in the perchlorate form. The resins were purified before use by treatment with warm, alkaline H_2O_2 followed by thorough washing with H_2O . Sodium perchlorate solutions which had been passed through the purified resins yielded cyclic voltammograms with no evidence of adsorbable or electroactive impurities.

Solutions of the complexes were frozen and stored at -70°C . No decomposition of frozen solutions kept at -70°C was evident for periods up to three weeks. The concentrations of pure complexes in the solutions were determined spectrophotometrically either directly by using the published extinction coefficients^{2, 8} or after conversion of the Cr(III) to CrO_4^{2-} .⁹

Polarograms and cyclic voltammograms of solutions of $\text{Cr}(\text{CN})_3$ invariably produced two, closely spaced waves with relative heights that depended on the amount of time that had elapsed since the preparation of the complex. With solutions that are stored for three weeks at 0°C the more anodic of the two waves becomes very prominent and only a vestigial remnant of the formerly sharp second wave remains. Such aged solutions also display spectral differences compared with freshly prepared solutions (fresh solutions: absorption maxima at 467 nm and 360 nm; aged solution: absorption maxima at 445 nm and 340 nm). Solutions stored at -70°C showed no similar spectral changes for storage periods as long as three weeks. We believe the double waves and spectral shifts are both reflections of the presence of varying amounts of polymeric chromium-cyanide species in these solutions. Insoluble polymeric precipitates are formed by $\text{Cr}(\text{CN})_3$ preparations upon repeated freezing and thawing of the solutions⁸ and the soluble precursors to these precipitates are the likely sources of the observed behavior.

Solutions of silver(I) and mercury(II) perchlorates were prepared by dissolving the respective oxides in small excesses of perchloric acid. 8 M NaClO₄ solutions were prepared by reacting 9.5 M perchloric acid with solid sodium carbonate heating the resulting solution on a steam bath overnight and filtering off the siliceous residue. The pH of the filtered solution was adjusted to be between 3 and 4 while stirring with nitrogen gas to remove CO₂.

For most of the electrochemical experiments the ionic strength was adjusted to 1.0 with NaClO₄. All solutions were prepared from triply-distilled water and deaerated with prepurified nitrogen.

Apparatus. -- The instrumental apparatus for cyclic voltammetry and chronocoulometry was essentially identical to one previously described.⁴ Potentials were measured with respect to a NaCl-saturated calomel electrode but are reported vs. the usual KCl-saturated calomel electrode (SCE). Controlled potential electrolysis over stirred mercury pool electrodes were performed with a Wenking potentiostat (Model TR).

The hanging mercury drop electrodes used for cyclic voltammetry and chronocoulometry were the commercially available Kemula Model (Brinkman Instruments, Inc.). The electrode area was 0.032 cm². All voltammograms were recorded at a potential scan rate of 10 volts per second.

Spectra were obtained with Cary 14 or Cary 11 spectrophotometers. Concentrations of the chromium compounds were determined by means of a Beckman DU spectrophotometer equipped with a Gilford Absorbance Indicator Model 220.

Results

Polarography and Cyclic Voltammetry. -- Polarograms and cyclic voltammograms of the three complexes, CrCN^{2+} , cis-Cr(CN)_2^+ and fac- Cr(CN)_3 , were recorded in sodium perchlorate supporting electrolytes at pH values below 3 because above pH 3 the cyanide ion released at the electrode surface caused the local pH to increase to values where the unreduced complexes were rapidly hydrolyzed and the waves collapsed.

The polarograms and voltammograms correspond to totally irreversible reductions with half-wave and peak potentials that are independent of pH between pH 0 and 3. For each complex the peak potentials become ca. 60 mV more cathodic for each decade increase in sweep rate indicating that the transfer coefficients, α , are close to 0.5 for all of the complexes. The half-wave and peak potentials for the three complexes as well as those for the hexaquo ion are collected in Table I.

With each complex an oxidation wave corresponding to the oxidation of Cr^{2+} to Cr^{3+} appeared at ca. 0 volts during the anodic half of the cyclic voltammogram. Thus, the reduction products in each case appear to be the same, namely Cr^{2+} and HCN. (Separate experiments with solutions containing the same concentrations of H^+ and CN^- showed that HCN does not produce an anodic wave at pH values between 0 and 2.5.)

TABLE I
HALF-WAVE AND PEAK POTENTIALS^a

Complex	$-E_{1/2}$, ^b V vs. SCE	$-E_p$, ^c V vs. SCE
Cr ³⁺	0.87	1.07
CrCN ²⁺	0.96 ^d	1.16
Cr(CN) ₂ ⁺	1.05	1.27
Cr(CN) ₃	1.15-1.20	1.36

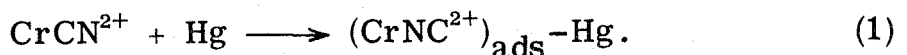
^a Supporting electrolyte was 1 M NaClO₄ adjusted to a pH between 1 and 2 with HClO₄.

^b DME characteristics: drop time = 4.6 sec (0 V);
m = 1.44 mg/sec.

^c Sweep rate = 10 volts/sec.

^d The same value of $E_{1/2}$ was obtained by Bustin and Earley (5) but the polarographic maxima they reported did not appear in our solutions.

The Search for Adsorption of the Complexes. -- One of our primary goals was to determine whether the cyano complexes of chromium(III) would mimic the behavior of the corresponding thiocyanato complexes by adsorbing on the surface of mercury electrodes.⁴ The electrochemical technique of potential-step chronocoulometry^{4, 10} was employed to search for any adsorption at a series of initial potentials between +0.2 and -0.7 volts. The known course of the homogeneous reaction between CrCN^{2+} and Hg^{2+} ^{1, 2} made it seem quite likely that if adsorption were to occur a linkage isomerization of the coordinated cyanide would be required:

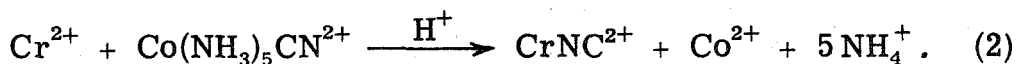


In contrast with the adsorption of most ions on mercury, a reaction such as (1) could proceed fairly slowly so that the mercury electrode was exposed to solutions of the complex for periods up to sixty seconds before the chronocoulometric determination of any adsorption was made. For both CrCN^{2+} and $\text{Cr}(\text{CN})_2^+$ the intercepts of the chronocoulometric plots (charge vs. $(\text{time})^{1/2}$) matched the corresponding intercepts in chromium-free solutions within 0.2-0.5 $\mu\text{C}/\text{cm}^2$ for every initial potential and the match was not affected by increasing the length of time the mercury surface was exposed to the solution. Thus, no evidence for adsorption of CrCN^{2+} or $\text{Cr}(\text{CN})_2^+$ was obtained. Solutions of $\text{Cr}(\text{CN})_3$ could not be examined for possible adsorption by chronocoulometry because of the small potential

separation between chromium(III) reduction and hydrogen ion reduction. However, electrocapillary curves (obtained from drop time measurements) for solutions of $\text{Cr}(\text{CN})_3$ showed no evidence of adsorption.

Electrochemical Preparation of the Linkage Isomer CrNC^{2+} .

-- The failure of CrCN^{2+} to adsorb on mercury electrodes despite its ready homogeneous reaction with Hg^{2+} might be attributed to a much weaker tendency for the electrode surface to provoke the formation of the linkage isomer according to reaction 1. To examine this possibility we sought to prepare solutions containing reasonable concentrations of the linkage isomer, CrNC^{2+} , and to examine its adsorption on mercury. An established route to CrNC^{2+} is known¹¹ that utilizes the following redox reaction:



The resulting isocyanochromium(III) complex has a half-life of several hundred seconds at 0°C and we expected to be able to monitor it electrochemically with cyclic voltammetry carried out immediately on solutions prepared by mixing Cr^{2+} and $\text{Co}(\text{NH}_3)_5\text{CN}^{2+}$.¹² However, attempts to observe the electrochemical reduction of CrNC^{2+} prepared by reaction 2 were thwarted by the presence in the product solution of an extremely active catalyst for hydrogen ion reduction. Reaction 2 needed to be carried out in solutions having pH values of 2 or less which yielded a large proton reduction wave commencing at about -0.7 volts.

This wave completely masked all electrode reactions occurring at more negative potentials such as the reduction of CrCN^{2+} and CrNC^{2+} .

In separate experiments it was possible to obtain an entirely similar catalytic wave by adding sodium cyanide to acidic solutions containing Co^{2+} (but not vice versa). This and other evidence indicates that the active catalyst is a cyano cobalt complex which is apparently generated in small quantities by reaction 2 even when excess Cr^{2+} is used. Although no waves could be observed that were attributable to reduction of Cr(III) species among the products of reaction 2, a new electroactive couple with anodic and cathodic waves centered about 0 volt is apparent just after reaction 2 is complete (Figure 1). This couple gradually disappears at a rate comparable to that observed by Birk and Espenson¹¹ for the isomerization reaction

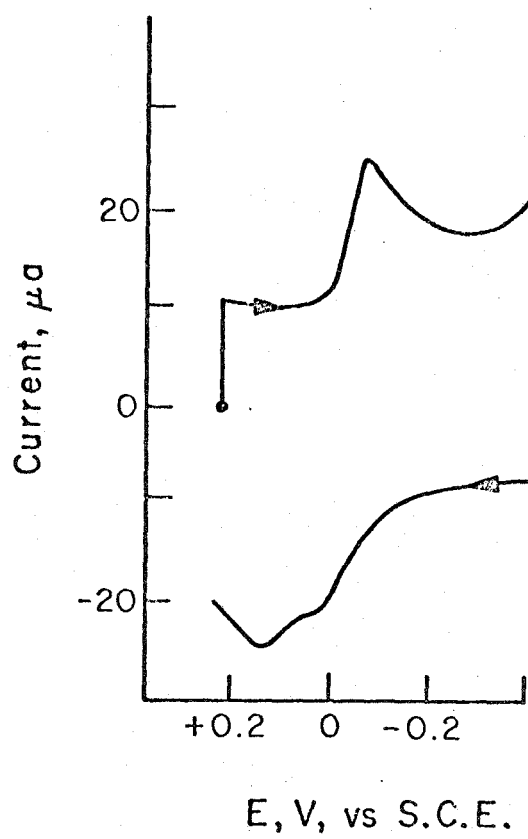


For reasons to be presented below the electrode processes that give rise to the waves in Figure 1 are believed to be reaction 4 and its reverse.



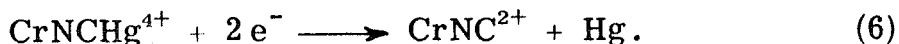
Because of the difficulties which ensue when reaction 2 is used to generate CrNC^{2+} a number of alternate routes for the preparation of the complex were investigated. The most suitable preparation for our purposes was based upon the homogeneous reaction between CrCN^{2+} and Hg^{2+} :^{1, 2}

Figure 1. -- Cyclic voltammogram obtained three minutes after reacting 5 mM Cr^{2+} with 4 mM $\text{Co}(\text{NH}_3)_5\text{CN}^{2+}$ in 0.1 M HClO_4 -0.9 M NaClO_4 at 2°C.





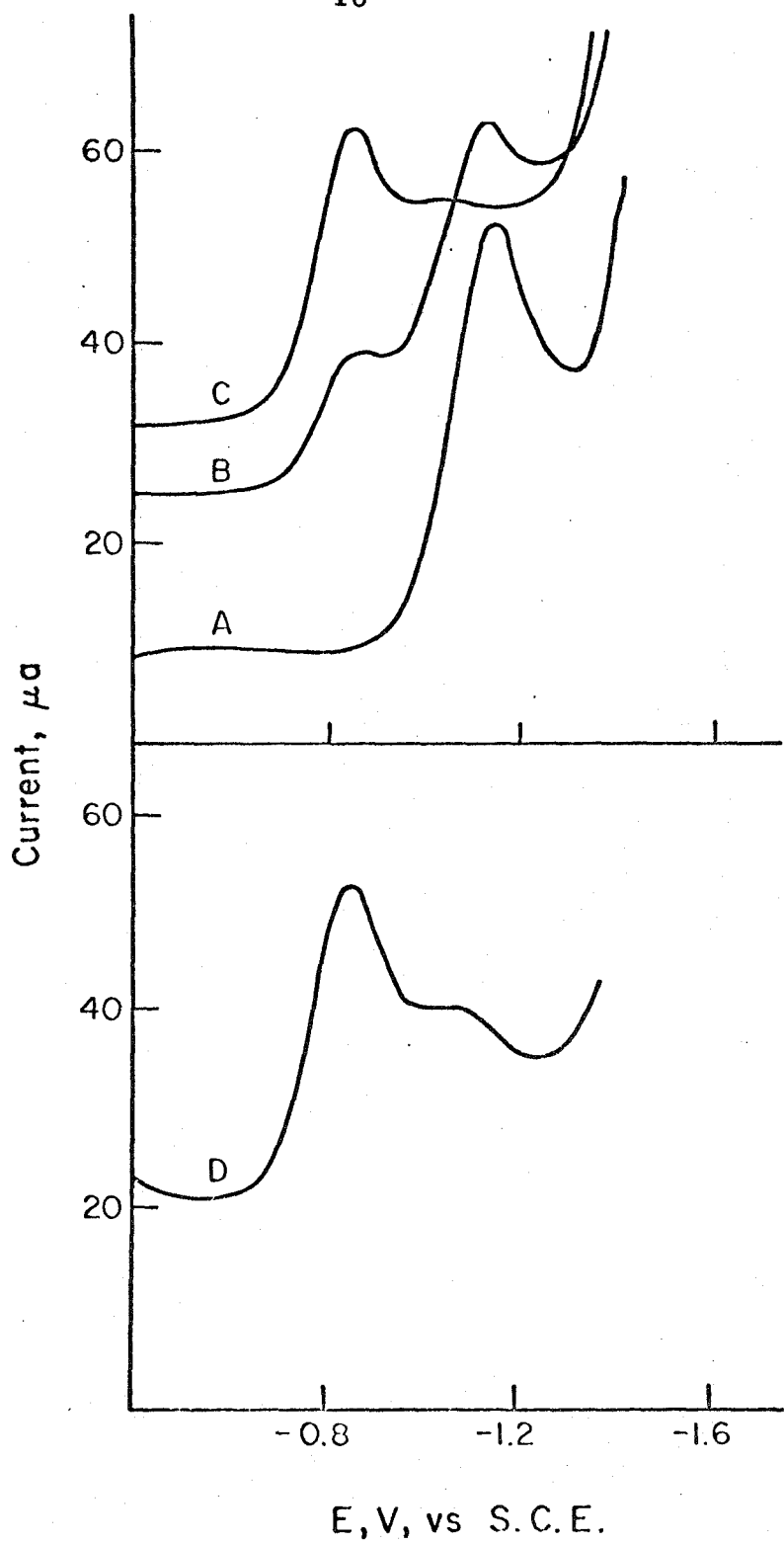
Electrochemical reduction of the Hg(II) in the binuclear cation produced in reaction 5 would be expected to yield CrNC^{2+} according to



If the reduction were carried out with a mercury electrode the metallic mercury would be incorporated into the electrode and the electrochemistry of the CrNC^{2+} produced at the electrode surface could readily be studied at the same electrode.

To test these expectations single sweep and cyclic voltammograms were recorded in solutions of CrCN^{2+} to which small excesses of Hg^{2+} were added. Figure 2 shows the results. When the current-potential curve is recorded within 20-30 seconds after addition of the Hg^{2+} to the solution of CrCN^{2+} reaction 5 has proceeded very little (the initial reaction rate is $9 \times 10^{-6} \text{ M sec}^{-1}$ under the conditions prevailing in Figure 2²) and the wave corresponding to reduction of unisomerized CrCN^{2+} (Curve A in Figure 2) is virtually unaffected by the presence of the mercury(II). When more time is allowed for reaction 5 to proceed the chromium(III) reduction wave splits into two waves: A new wave with a peak potential of -0.9 volt grows at the expense to the original wave at -1.1 volt. This process is shown in Curves B and C of Figure 2 which were obtained by maintaining the electrode for 1-2 seconds at an initial potential (-0.4 volt) where

Figure 2. -- Cathodic voltammograms of:
A, 1 mM CrCN^{2+} ; B, 1 mM CrCN^{2+} + 2 mM Hg^{2+} , 2 min
after mixing; C, as in B, 10 min after mixing;
D, 1.15 mM CrCN^{2+} + 0.58 mM Ag^+ 15 min after mixing.
Supporting electrolyte: 0.1 M HClO_4 -0.9 M NaClO_4 ;
T = 22°C.



the reduction of CrNCHg^{2+} is diffusion controlled before commencing the potential scan in order to allow the current arising from mercury(II) reduction to decay sufficiently so that the relative magnitudes of the subsequent waves are more readily measured. Note that ten minutes after mixing (Curve C, Figure 2) the new wave at -0.9 volt has become the major wave with only a small remnant remaining of the wave corresponding to the reduction of CrCN^{2+} .

A number of lines of evidence can be cited to support the assertion that the new wave at -0.9 volt is due to the reduction of the isocyno complex:



It was verified that the product of the reduction reaction for this wave is Cr^{2+} by reversing the direction of the potential scan in a solution containing chloride ion and observing the characteristic chloride-catalyzed Cr^{2+} oxidation wave¹³ during the anodic scan. If the direction of the potential scan from -0.4 volt is anodic rather than cathodic with a solution such as the one that gave curve C in Figure 2, the same pair of anodic-cathodic waves (centered at 0 volts) is found that was obtained when CrNC^{2+} was generated via reaction 2 (Figure 1). In addition, the rate at which the peak currents grow following the addition of Hg^{2+} matches the growth rate of the new cathodic wave at -0.9 volt, as it should if both the anodic and cathodic waves involves diffusion to the electrode of the same reaction product, CrNC^{2+} .

Silver ion also reacts with CrCN^{2+} to yield spectral changes resembling those obtained with Hg^{2+} : A mixture containing one mole of Ag^+ per mole of CrCN^{2+} yields a spectrum with maxima at 556 and 399 nm. The same mixture prepared with Hg^{2+} has maxima at 565 and 401 nm^{1, 2} and pure CrCN^{2+} has maxima at 525 and 393 nm.⁸ Reduction of the Ag^+ adducts at mercury electrodes (the Ag^+ is reduced to silver metal which dissolves in the mercury) followed by a linear potential scan yields the same cathodic and anodic voltammograms that are obtained when Hg^{2+} is used. Thus, the same product, namely CrNC^{2+} , appears to result from the reduction of the heavy metal cation in both adducts.

CrCN^{2+} reacts considerably faster with Ag^+ than with Hg^{2+} and the resulting complex appears to aquate much less rapidly (e. g., negligible aquation of the Ag^+ complex during a period when 50% of the Hg^{2+} complex aquates). For these reasons Ag^+ was utilized most often to generate CrNC^{2+} at electrode surfaces.

Composition and Stability of the Hg^{2+} and Ag^+ Adducts. --

The voltammetric wave for reduction of CrCN^{2+} is converted almost completely into the wave corresponding to CrNC^{2+} reduction in solutions containing only 0.5 mole of Hg^{2+} or Ag^+ per mole of CrCN^{2+} (Figure 2, Curve D). This observation indicated that the formation of the heavy metal adducts in solutions not containing excesses of the heavy metal ions might involve a different stoichiometry than the simple one-to-one complexation of reactions such as 5. Espenson and Bushey² alluded to the same possibility but did not pursue it quantitatively.

Potentiometric titration of CrCN^{2+} solutions with Hg^{2+} or Ag^+ using Hg or Ag electrodes, respectively, were therefore performed to investigate the stoichiometries of the adduct formation reactions at low concentrations of heavy metal.

Figure 3 shows some typical titration curves. The rate of reaction between CrCN^{2+} and the heavy metal ions is fairly slow so that several minutes were required before steady potential readings were obtained after each addition of reactant. The rather long times required for the adduct formation to reach equilibrium caused no problems in the case of the Ag^+ -adduct because of its much slower aquation rate. With the Hg^{2+} -adduct, however, considerable aquation occurred during the time (~ 60 minutes) required to complete a titration. To overcome this problem the complete titration curve was assembled from a series of titrations which commenced with successively higher amounts of added mercury(II). That the steady potentials eventually achieved corresponded to a true equilibrium was supported by the fact that the inflection points in the titration curves occurred at the same stoichiometric ratio of reactants regardless of the direction in which titration was performed.

The inflection points in the potentiometric titration curves correspond to the formation of the adducts $(\text{CrNC})_2\text{Hg}^{6+}$ and $(\text{CrNC})_2\text{Ag}^{5+}$. Additional evidence supporting this trinuclear stoichiometry for the adducts was obtained from amperometric titrations. Figure 4 shows the current at a dropping mercury electrode held at -0.5 volt where no reduction of any Cr(III) species

Figure 3. -- Potentiometric titrations of CrCN^{2+} with Hg^{2+} and Ag^{1+} .

1 -- 124.5 μ moles of CrCN^{2+} in 25 ml of 0.1 M HClO_4 -0.9 M NaClO_4 titrated with 0.030 M Ag^{1+} .

2 -- 126 μ moles of CrCN^{2+} in 25 ml of 0.1 M HClO_4 -0.9 M NaClO_4 titrated with 0.030 M Hg^{2+} .

The abscissa gives the moles of heavy metal cation added per mole of CrCN^{2+} initially present.

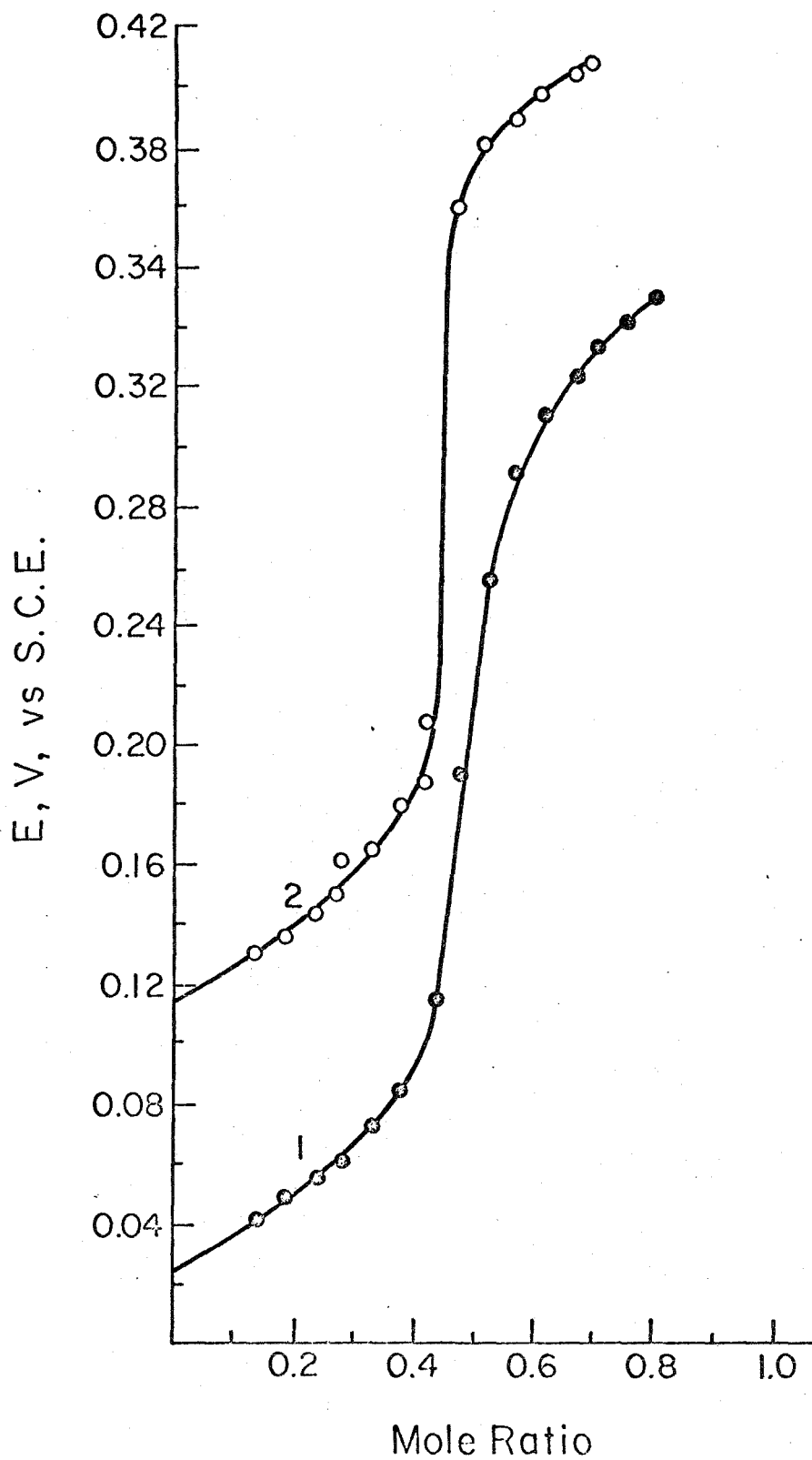
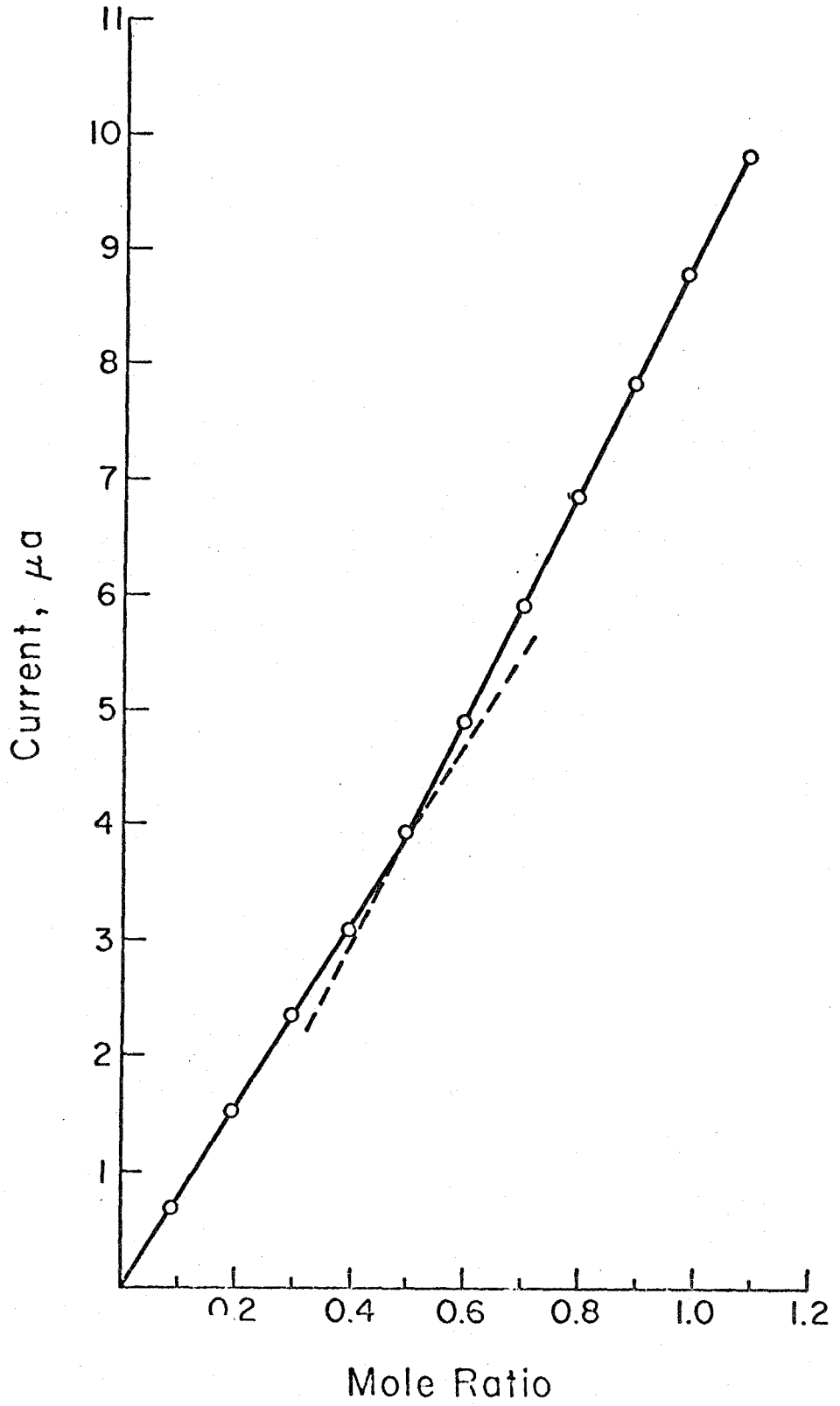
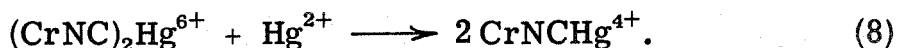


Figure 4. -- Amperometric titration of CrCN^{2+} with Hg^{2+} . 60.8 μ mole of CrCN^{2+} in 40 ml of 0.1 M HClO_4 -0.9 M NaClO_4 titrated with 0.030 M Hg^{2+} . The d. m. e. was maintained at -0.5 V vs. s. c. e. The abscissa gives the moles of Hg^{2+} added per mole of CrCN^{2+} initially present.



occurs but the Hg(II) contained in the adduct is reduced. The titration utilizes the fact that the diffusion coefficient of $(\text{CrNC})_2\text{Hg}^{6+}$ is significantly smaller than those of CrNCHg^{4+} and Hg^{2+} . During the first half of the titration the current increases at a rate proportional to the concentration of $(\text{CrNC})_2\text{Hg}^{6+}$. During the second half of the titration the current increases more rapidly because reaction 8 begins to become important and leads to the partial conversions of the $(\text{CrNC})_2\text{Hg}^{6+}$ to CrNCHg^{4+}



The intersection of the two linear segments should correspond to the maximum concentration of $(\text{CrNC})_2\text{Hg}^{6+}$. The fact that it occurs at a stoichiometric ratio of 0.5 Hg^{2+} per CrCN^{2+} is strong evidence that this is the mole ratio in the adduct.

An amperometric titration with the Ag^+ - CrCN^{2+} system could not be performed in the same way because of interference by polarographic maxima. To avoid the maxima a solution of Ag^+ was titrated with CrCN^{2+} and the electrode was maintained at -0.8 volt where both CrNC^{2+} and the Ag^+ -adduct but not CrCN^{2+} contribute to the diffusion limited current. The first intersection point appeared at a Ag(I) to Cr(III) mole ratio somewhat less than the value expected for formation of CrNCAg^{3+} but the second intersection occurred at a mole ratio of Cr(III) per Ag(I) corresponding to quantitative formation of $(\text{CrNC})_2\text{Ag}^{5+}$.

The potentiometric titration data can be utilized to evaluate equilibrium quotients for formation of the adducts. Analysis of the

data by the procedure outlined in the appendix produced the equilibrium quotients listed in Table II

TABLE II
EQUILIBRIUM QUOTIENTS FOR ADDUCTS WITH Hg^{2+} AND Ag^+

Reaction	Equilibrium Quotient
(I) $\text{CrCN}^{2+} + \text{Hg}^{2+} = \text{CrNCHg}^{3+}$	$Q_{\text{I}} = 3 \pm 0.7 \times 10^7$
(II) $\text{CrCN}^{2+} + \text{HgCNCr}^{4+} = (\text{CrNC})_2\text{Hg}^{6+}$	$Q_{\text{II}} = 4 \pm 2 \times 10^7$
(III) $\text{CrCN}^{2+} + \text{Ag}^+ = \text{CrNCAg}^{3+}$	$Q_{\text{III}} = 5 \pm 2 \times 10^5$
(IV) $\text{CrCN}^{2+} + \text{AgCNCr}^{3+} = (\text{CrNC})_2\text{Ag}^{5+}$	$Q_{\text{IV}} = 11 \pm 10 \times 10^4$

Protonation of CrNC^{2+} . -- In contrast with the behavior of CrCN^{2+} , the cathodic voltammograms for the complex generated from either the Hg^{2+} or the Ag^+ adduct display peak potentials that are pH dependent. The existence of this pH dependence and the fact that both heavy metal adducts lead to products with the same pH dependence are taken as added evidence that the same species, CrNC^{2+} , is being produced in both cases. Figure 5 shows the experimentally observed pH dependence along with that to be expected¹⁴ if the electrode reaction were preceded by protonation of the isocyano complex:

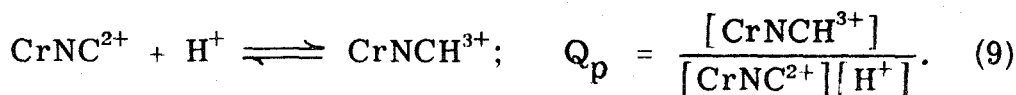


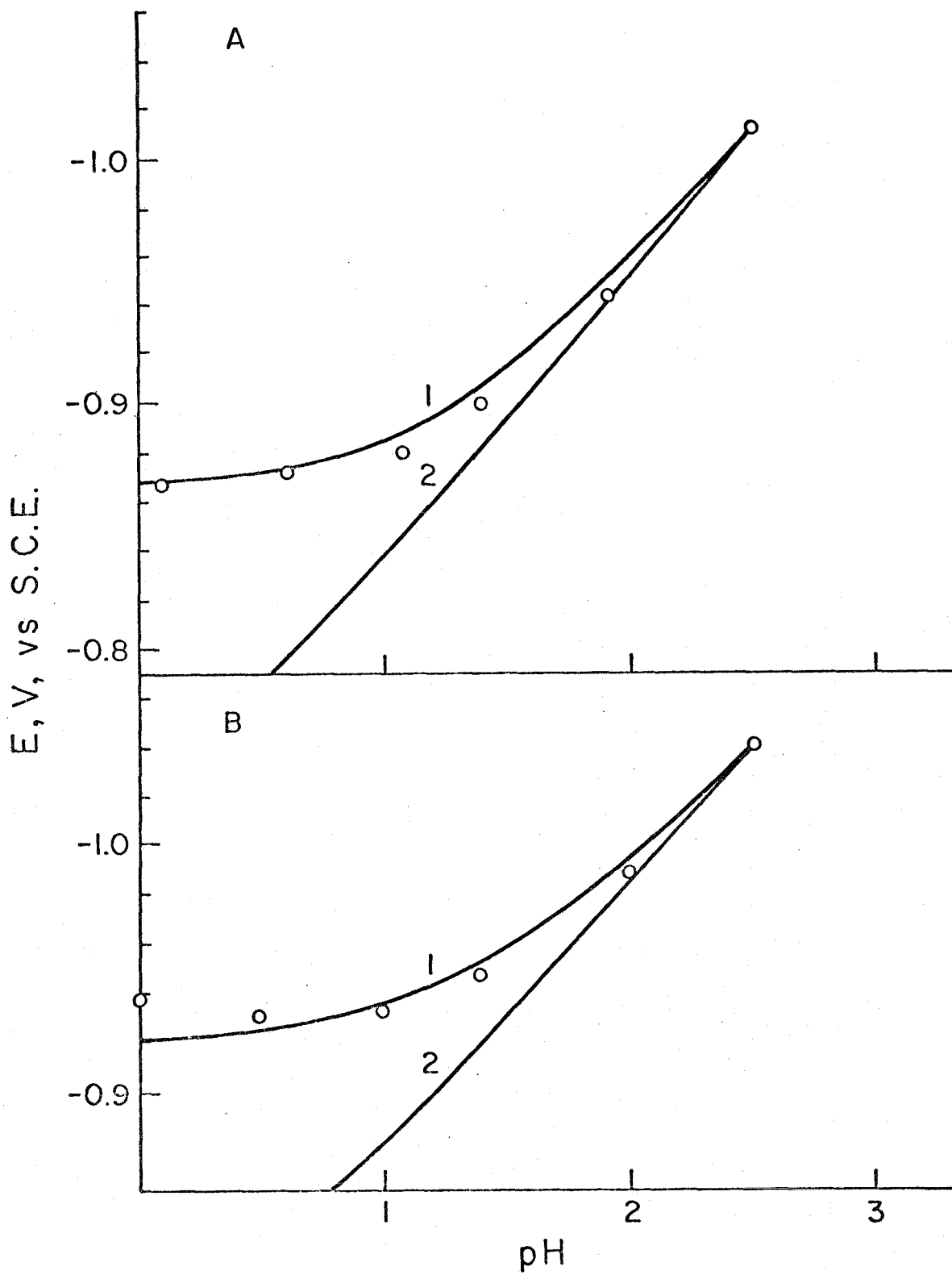
Figure 5. -- pH Dependence of voltammetric peak potentials, for reduction of CrNC^{2+} . The plotted points are the experimental peak potentials. The curves were calculated from a simplified version of equation 75 of reference 14:

$$E = E_r - \frac{RT}{\alpha F} \left[\ln \left(\frac{Q_p [H^+]}{1 + Q_p [H^+]} \right) - \ln \left(\frac{Q_p [H^+]_r}{1 + Q_p [H^+]_r} \right) \right]$$

where E_r is the peak potential when $[H^+] = [H^+]_r$. The peak potential at the highest pH was chosen as E_r . The values of Q_p used to calculate curves 1, A and B were obtained from least-squares fitting of the data to this equation. Curves 2, A and B were calculated using the estimate (11), $Q_p = 0.94$. The supporting electrolyte concentration was maintained at 1 M with NaClO_4 .

A -- 25°C

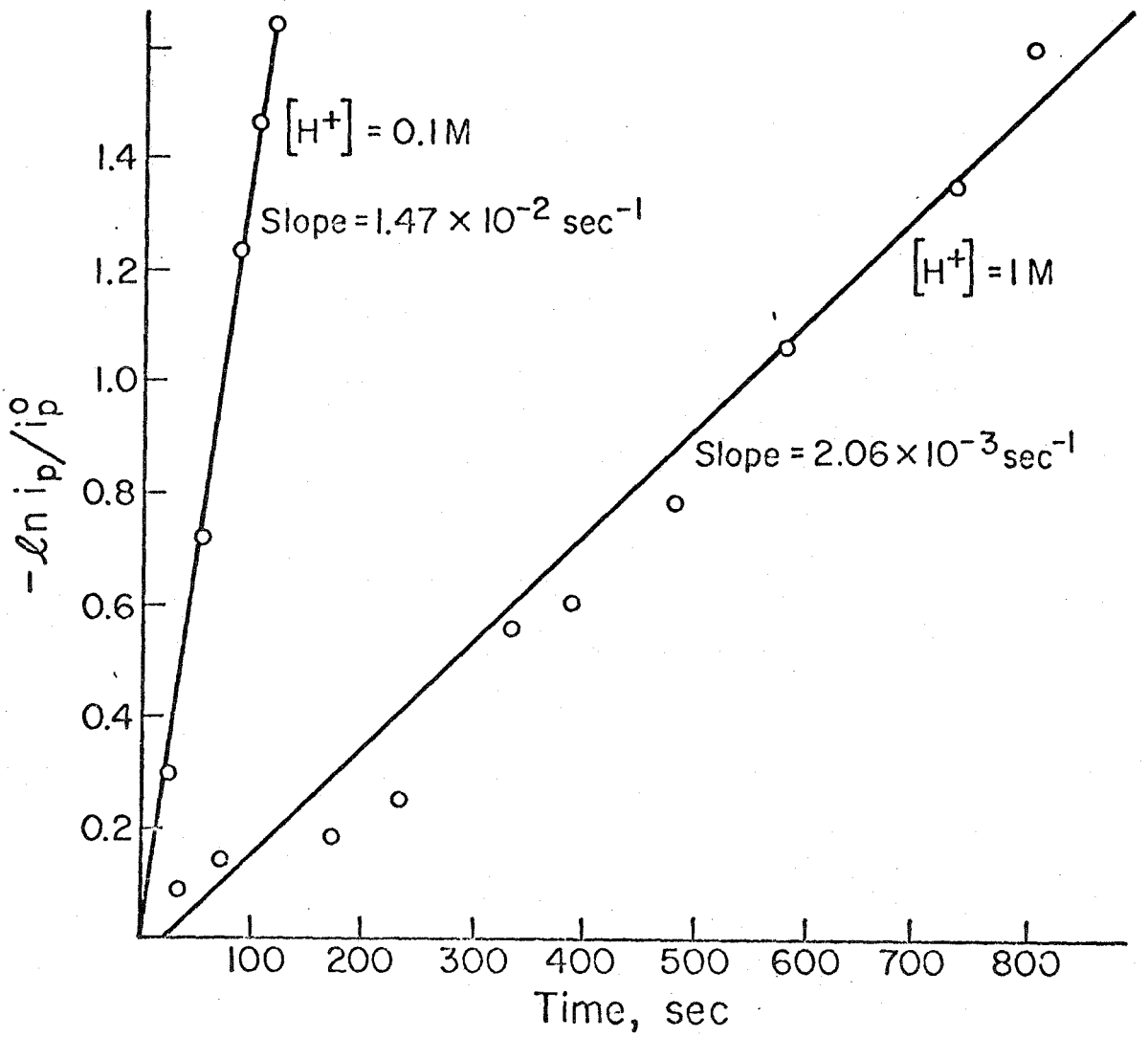
B -- 2°C



Curve 2 in Figure 5A was obtained by using Birk and Espenson's kinetically estimated value for the equilibrium quotient for reaction 9, $Q_p = 0.94$.¹¹ Curve 1 in Figure 5A which gives the best fit of the experimental data to the appropriate theoretical equation¹⁴ was obtained by using a value of 18.7 for Q_p . Thus, these data suggest that Q_p may be considerably larger than the previous estimate.¹¹ A second series of voltammograms was recorded at 2°C where the isocyno complex is more stable. The data, shown in Figure 5B, indicate that at 2°C Q_p is ca. 28.6.

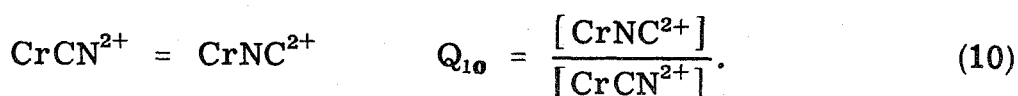
The product of the values of Q_I and Q_{II} in Table II is slightly larger than the corresponding formation quotient for $HgCl_2$ but much smaller than the quotient for HgI_2 .¹⁵ It follows that excess iodide ion but not excess chloride ion should decompose solutions of $Hg(CNCr)_2^{6+}$ into $CrNC^{2+}$ and the mercury halide complex. These expectations were borne out in experimental tests and the rapid reaction between $Hg(CNCr)_2^{6+}$ and excess iodide ion was used to generate homogeneous solutions of $CrNC^{2+}$ which were used to measure the kinetics of its re-isomerization to $CrCN^{2+}$ at 2°C. (At room temperature the rate was inconveniently rapid.) The rate was followed by measuring the peak currents of the voltammetric waves for reduction of the $CrNC^{2+}$ remaining at various time intervals after addition of the iodide. Rate data at two different pH values are plotted in Figure 6. The pH dependence of this isomerization rate has been explained by Birk and Espenson as arising from the protonation of $CrNC^{2+}$ to form $CrNCH^{3+}$ which isomerizes much more slowly.¹¹ Accordingly, they

Figure 6. -- Rate of conversion of CrNC^{2+} into CrCN^{2+} at $\text{pH} = 0$ and $\text{pH} = 1.0$. The peak currents, i_p , corresponding to the reduction of CrNC^{2+} were measured and the ratio of i_p at each time to the first value of i_p , i_p^0 , was used in plotting the ordinate. (Solutions were prepared by reacting 2 mM Hg^{2+} with 2 mM CrCN^{2+} at 22°C , waiting 10 minutes then cooling to 2°C and making the solution 25 mM in NaI .) The supporting electrolyte concentration maintained at 1 M with NaClO_4 . (Data point at 1050 sec, $-\ln i_p/i_p^0 = 2.2$, not shown but included in data analysis for $1 \text{ M } [\text{H}^+]$.)



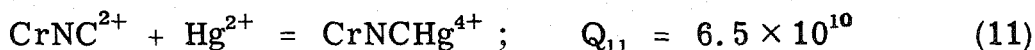
write $k_{\text{obs}} = \left(\frac{1}{1 + Q_p [\text{H}^+]} \right) k_i$ where k_{obs} is the observed isomerization rate constant, Q_p is the protonation quotient (reaction 9), and k_i is the rate constant for isomerization of the unprotonated complex. The ratio of the two values of k_{obs} obtained from the slopes of the lines in Figure 6 yields a value of 21 for Q_p at 2°C. The reasonable agreement between these estimates of Q_p derived from the pH dependences of both the voltammetric peak potentials (Figure 5) and the isomerization kinetics (Figure 6) supports the reliability of the larger values for Q_p resulting from these measurements. Accordingly, the estimate of the protonation quotient obtained at 22°C, $Q_p = 18.7$, will be used in the discussion to follow.

Spontaneous Isomerization of CrCN^{2+} . -- Espenson and Birk¹⁶ give 0.048 as an estimate of the upper limit for the equilibrium quotient for reaction 10:



This value is large enough for the concentration of the isocyano isomer present at equilibrium in a sufficiently concentrated solution of CrCN^{2+} to be determined electrochemically. For example, a 10 mM solution of CrCN^{2+} should contain 0.48 mM CrNC^{2+} which is a concentration large enough to yield detectable voltammetric waves corresponding to the isocyano isomer as in Figures 1 and 2.

Figure 7 contains a set of voltammograms obtained with a 10 mM solution of CrCN^{2+} at several pH values. The expected cathodic and anodic waves corresponding to CrNC^{2+} are observed and their peak currents are used in Table III to evaluate the equilibrium quotient for spontaneous linkage isomerization, Q_{10} . The average value obtained in this way, $Q_{10} = 4.8 \pm 1 \times 10^{-3}$, is compatible with, but about ten times smaller than the previously estimated upper limit.¹⁶ Combining this value of Q_{10} with Q_7 , the equilibrium quotient for reaction 5, leads to a value for the equilibrium quotient for the binding of Hg^{2+} to the isocyanochromium(III) complex:



This value is consistent with the estimated lower limit on this quotient of 2×10^6 given by Espenson and Bushey.²

Nonadsorption of CrNC^{2+} on Mercury. -- Of the two methods described for generating significant concentrations of CrNC^{2+} at the surface of a mercury electrode (electroreduction of the heavy metal adducts or reaction of the Hg^{2+} -adduct with excess iodide ion) the electroreduction route was selected for experiments designed to search for possible adsorption of CrNC^{2+} in order to eliminate interference from competitive adsorption by iodide. It was necessary to modify the usual chronocoulometric procedure for measurement of adsorbed, electroactive species.¹⁰ First, the potential of the mercury

Figure 7. -- Voltammograms of a 10 mM
CrCN²⁺ solution at:
1 -- pH = 2; 2 -- pH = 1; 3 -- pH = 0.5; 4 -- pH = 0.
The supporting electrolyte also contained 0.9 M
NaClO₄ (except 4); T = 22°C.

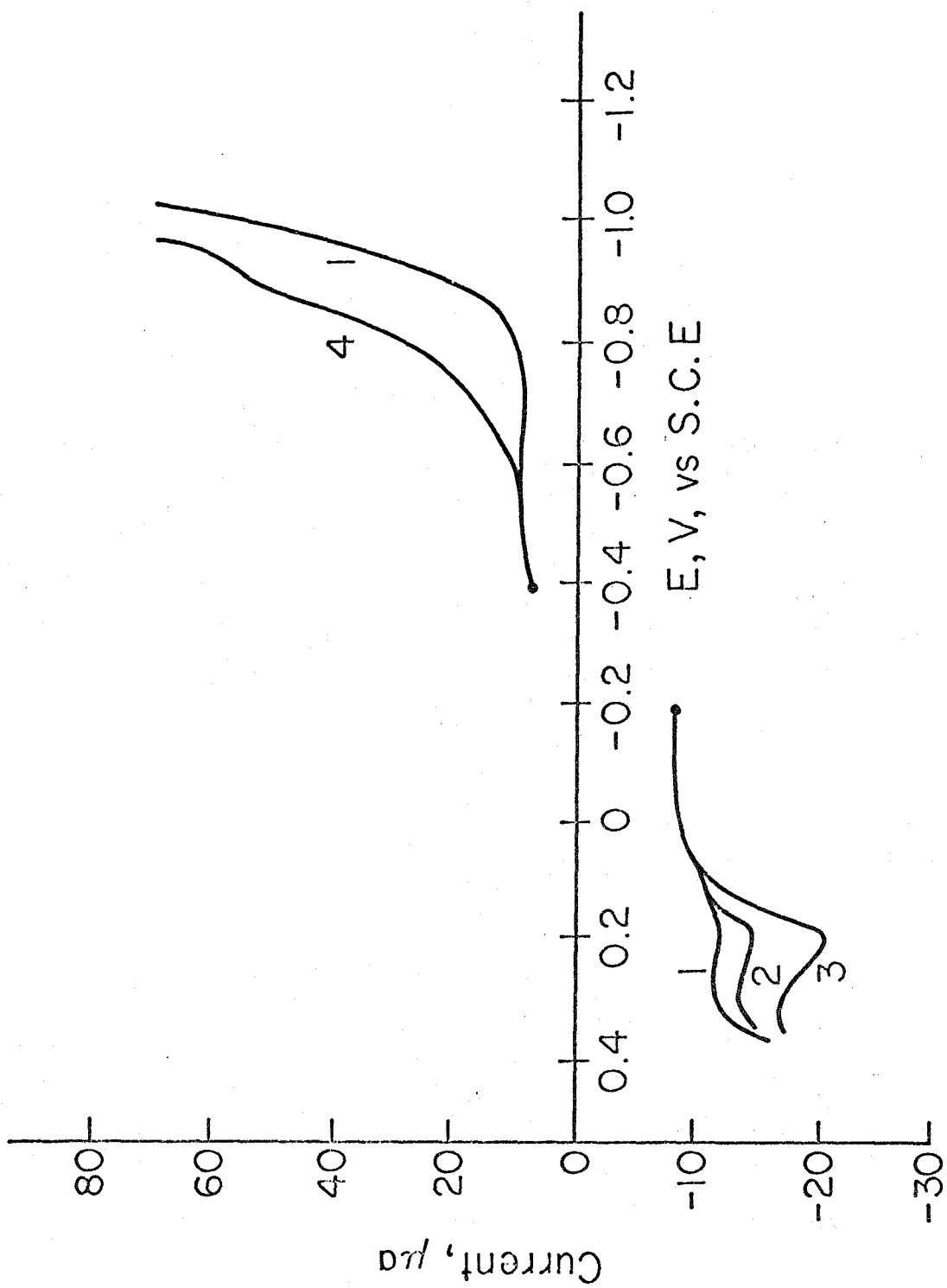


TABLE III
ESTIMATION OF Q_{10} FROM PEAK CURRENTS FOR
Hg OXIDATION (REACTION 4) AND CrNC^{2+} REDUCTION
IN A 10 mM SOLUTION OF CrCN^{2+}

pH	Anodic peak current, μA	Cathodic peak ^a current, μA	$Q_{10} \times 10^3$ ^b
2	4	c	7.2
1	6	c	4.7
0.5	11	c	3.7
0	35		4.4
0	—	34	<u>4.2</u>
			Average = 4.8 ± 1

^a Corrected for the current resulting from reduction of CrCN^{2+} at the potential where the peak current was measured.

^b Calculated from $i_p = i_p^0 \alpha$, where i_p is the observed peak current (anodic or cathodic), i_p^0 is the total peak current corresponding to the reduction of all isomers of Cr(III) present (480 μA for the experimental conditions employed), and α is the fraction of the Cr(III) present in the two isocyno forms: $\text{CrNC}^{2+} + \text{CrNCH}^{3+}$;

$$\alpha = \frac{Q_{10} (Q_p [\text{H}^+] + 1)}{1 + Q_p Q_{10} [\text{H}^+] + Q_{10}}$$

^c The small cathodic wave was too close to the main reduction wave of CrCN^{2+} for accurate estimation of the peak current at these pH values.

electrode was stepped to a value where the Hg(II) in the $\text{Hg}(\text{CNCr})_2^{6+}$ complex was reduced to metallic mercury and the surface of the electrode was exposed to the CrNC^{2+} that resulted. After sufficient isocyano complex had been generated at the electrode to yield a measurable adsorption if it were adsorbed, the electrode potential was stepped to a value where the CrNC^{2+} (as well as the small amounts of CrCN^{2+} produced by re-isomerization) was reduced to Cr^{2+} along with the additional amount of $\text{Hg}(\text{CNCr})_2^{6+}$ that continued to diffuse to the electrode. Appropriate analysis¹⁷ of the charge-time behavior obtained from the sum of the two electrode reactions leads to linear chronocoulometric plots with intercepts that measure the amount of adsorbed CrNC^{2+} , if any. The intercepts obtained with solutions containing no CrCN^{2+} matched those obtained in the presence of chromium within $0.2 \mu\text{C}/\text{cm}^2$ indicating that no more than 2×10^{-12} moles/ cm^2 of the complex is adsorbed. Similar results were obtained at both 2° and 25°C and when Ag^+ was substituted for Hg^{2+} in generating the CrNC^{2+} . Under the experimental conditions employed the amount of CrNC^{2+} produced at the electrode surface was three to four times more than would be needed to form a monolayer on the electrode, i. e., an ample amount to have resulted in adsorption if it were favored.

The lack of adsorption of CrNC^{2+} on mercury contrasts with the behavior of CrNCS^{2+} although the latter cation is only weakly adsorbed.⁴ Much stronger adsorption is obtained with $\text{Cr}(\text{NCS})_2^+$ and

$\text{Cr}(\text{NCS})_3^4$ and it therefore seemed desirable to try to prepare the isocyano analogs of the di- and tri-thiocyanato complexes to see if they were adsorbed in detectable amounts.

Electrochemical Generation of $\text{Cr}(\text{NC})_2^+$ and NCCrNC^+ . --

When Hg^{2+} or Ag^+ is added to solutions of $\text{Cr}(\text{CN})_2^+$ new voltammetric reduction waves slowly develop as the original wave corresponding to the reduction of $\text{Cr}(\text{CN})_2^+$ decays (Figures 8, 9). (New anodic waves corresponding to mercury oxidation in the presence of the isocyano chromium(III) complexes also appear but they were not extensively investigated.) The two cathodic waves developed by the addition of Hg^{2+} appear at potentials on either side of the single wave that develops in solutions of CrCN^{2+} . Figure 8 shows the temporal development of the two waves. Wave A appears first. Wave B develops somewhat later and continues to increase in magnitude even after the original $\text{Cr}(\text{CN})_2^+$ reduction wave, C, has disappeared completely, which indicates that wave B results from a continuing reaction between the Hg^{2+} added and the species responsible for wave A. At 25°C approximately 20 minutes are required for the wave heights to stop changing and their final relative magnitudes depend upon the mole ratio of Hg^{2+} to $\text{Cr}(\text{CN})_2^+$ employed; wave B increases and wave A decreases in magnitude as the mole ratio is increased from 1 to 2.0.

Figure 8. -- Voltammograms of:

1 -- 1 mM $\text{Cr}(\text{CN})_2^{1+}$; 2 -- 1 mM $\text{Cr}(\text{CN})_2^{1+}$ + 1 mM Hg^{2+} ,

3 min after mixing; 3 -- as in 2, 20 min after mixing--

no further changes occur. Supporting electrolyte:

0.1 M HClO_4 -0.9 M NaClO_4 .

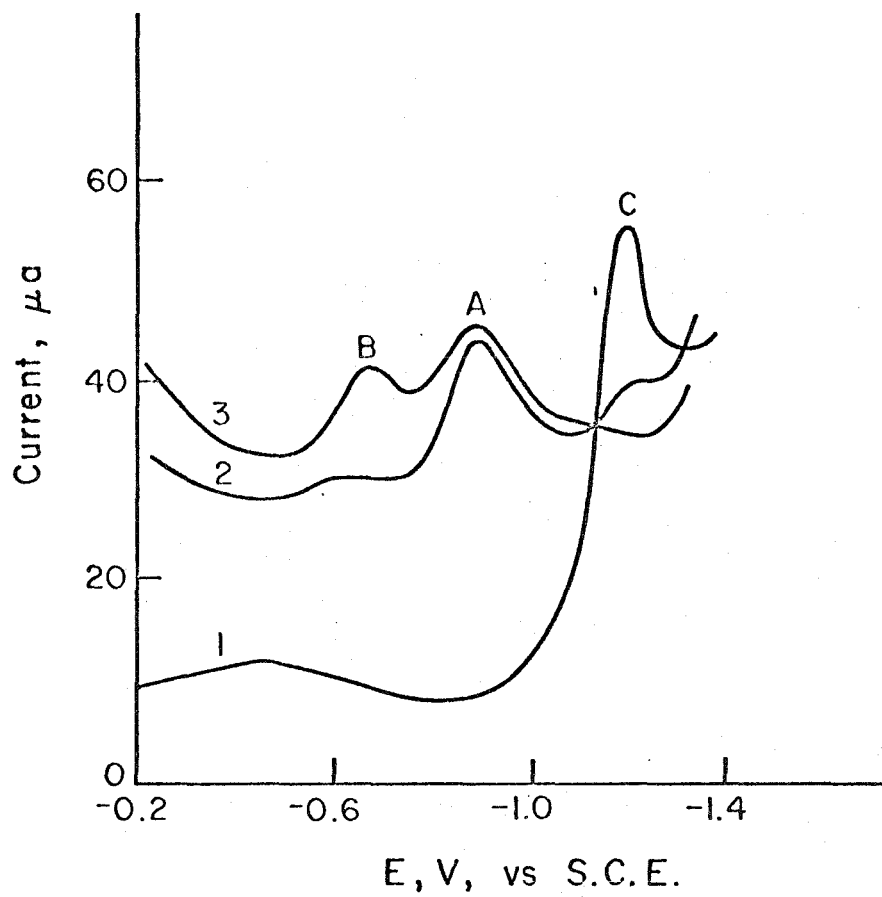


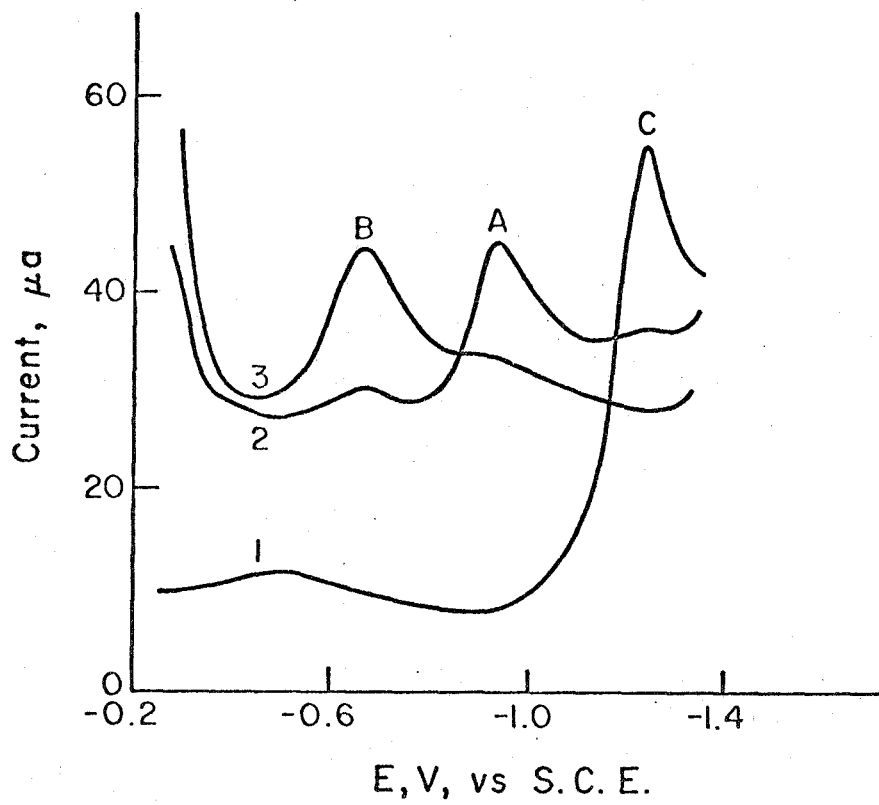
Figure 9. Voltammograms of:

1 -- 1 mM $\text{Cr}(\text{CN})_2^{1+}$; 2 -- 1 mM $\text{Cr}(\text{CN})_2^{1+}$ + 1 mM Ag^{1+}

15 - 30 sec after mixing; 3 -- as in 2, 9 min after mixing.

Supporting electrolyte: 0.1 M HClO_4 -0.9 M NaClO_4 ;

T = 2°C.



Soon after the relative wave heights become stable the peak potential of wave A begins to shift in an anodic direction and eventually moves to the potential characteristic of CrNC^{2+} . This suggests that mercury-induced aquation of $\text{Cr}(\text{CN})_2^+$ is proceeding as does the fact that the shift in peak potential occurs more rapidly at higher concentrations of Hg^{2+} .

Silver ion reacts with $\text{Cr}(\text{CN})_2^+$ much more rapidly than does Hg^{2+} and with one mole of Ag^+ added to each mole of $\text{Cr}(\text{CN})_2^+$ at 25°C there appears only a single new cathodic wave, identical to wave B obtained from Hg^{2+} addition (Figure 8). By cooling the solution, however, the intermediate appearance of a second new wave, apparently identical to wave A in Figure 8, becomes visible (Figure 9). In fact, at 2°C , the second wave, A, develops within 10-20 seconds and several minutes are required before wave A decays and wave B appears. In contrast to the behavior with Hg^{2+} , Ag^+ leads eventually to an essentially complete conversion to wave B even at a mole ratio of one Ag^+ per $\text{Cr}(\text{CN})_2^+$.

The potentials of both waves A and B are pH dependent as is true of the wave for CrNC^{2+} but not of the waves for CrCN^{2+} or $\text{Cr}(\text{CN})_2^+$ suggesting that the two waves correspond to the complexes NCCrNC^+ and $\text{Cr}(\text{NC})_2^+$. To examine the stoichiometry of the adduct-forming reaction, potentiometric titrations such as those performed with the monocyano complex were attempted at 25°C where the rate of adduct formation is reasonably rapid. The aquation rate of the complexes in the presence of mercury(II) proved to be too rapid for

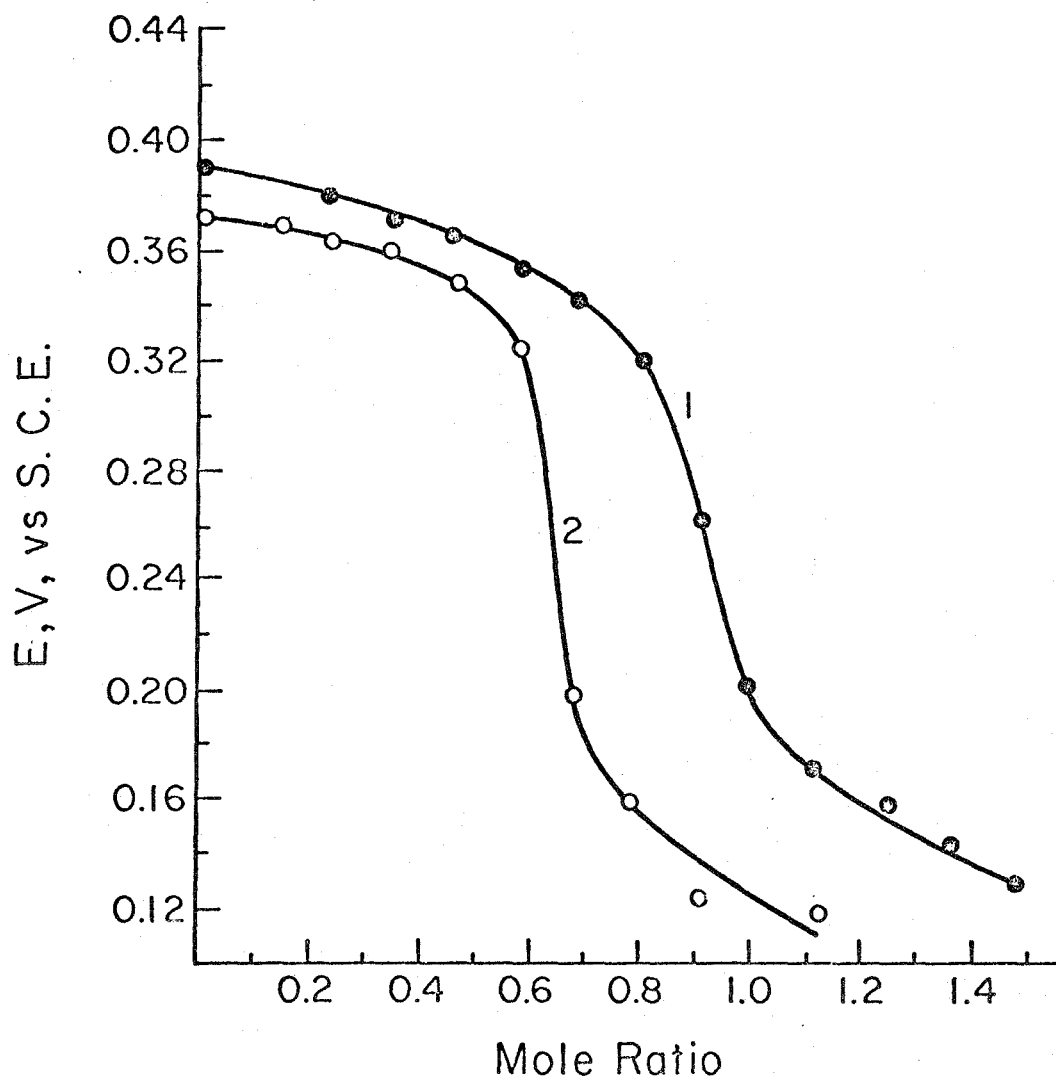
the attainment of steady potentials but successful titrations were obtained with the less rapidly aquating silver adducts. Curve 1 in Figure 10 shows the titration of Ag^+ with $\text{Cr}(\text{CN})_2^+$. The inflection in the curve occurs at a mole ratio of 0.9 indicating a stoichiometry close to one mole of $\text{Cr}(\text{CN})_2^+$ per mole of Ag^+ which contrasts with the two-to-one stoichiometry obtained for the same titration with CrCN^{2+} (Figure 3).

The voltammograms obtained from solutions containing equal molar quantities of Ag^+ and $\text{Cr}(\text{CN})_2^+$ display only the single wave, B. However, as more $\text{Cr}(\text{CN})_2^+$ is added wave B is decreased in magnitude and wave A develops. This behavior is in accord with that expected if $\text{Cr}(\text{NC})_2^+$ were generated from solutions containing molar excesses of Ag^+ over the complex but NCCrNC^{2+} resulted when the converse were true.

The slow rates of attainment of equilibria and the multiplicity of species present prevented the use of the potentiometric titration data for evaluation of equilibrium quotients for the formation of these heavy metal adducts with the dicyanochromium(III). It was possible, however, to obtain estimates of the relative stabilities of the mercury(II) and silver(I) adducts by comparing the equilibrium voltammograms obtained with the two heavy metals. The curves numbered 3 in Figures 8 and 9 show such a comparison and lead to the conclusion that the stability of the silver(I) precursor to the electrogenerated $\text{Cr}(\text{NC})_2^+$ ion (responsible for wave B) is greater than that of its mercury(II) counterpart.

Figure 10. -- Potentiometric titrations of Ag^{1+} with $\text{Cr}(\text{CN})_2^+$ and $\text{Cr}(\text{CN})_3$.

1 -- 45 μ mole of Ag^+ in 29 ml of 0.1 M HClO_4 -0.9 M NaClO_4 titrated with 0.0258 M $\text{Cr}(\text{CN})_2^{1+}$; 2 -- 30 μ mole of Ag^{1+} in 33 ml of 0.1 M HClO_4 - 1 F NaClO_4 titrated with 0.0171 F $\text{Cr}(\text{CN})_3$. The abscissa gives the moles of Cr(III) added per mole of Ag(I) present.



Qualitative experiments showed that small excesses of iodide but not chloride ion decomposed the heavy metal adducts and thus eliminated waves A and B (Figures 8 and 9) from voltammograms. The adducts formed with the dicyano complex therefore are not very much more stable than those obtained with the monocyano complex.

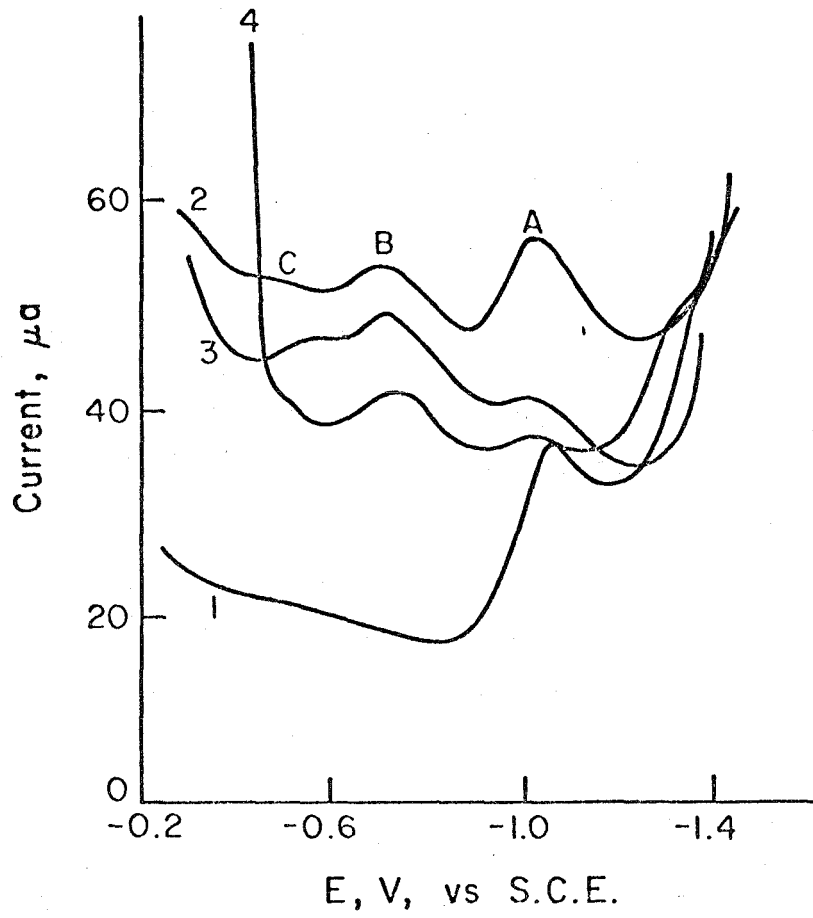
Chronocoulometry was used to investigate the possible adsorption of the two isocyano complexes generated at the electrode surface by reduction of the heavy metal adducts. The silver(I) adduct was employed to obtain $\text{Cr}(\text{NC})_2^+$ and the mercury(II) adduct to obtain NCCrNC^+ . Neither of these two complexes were adsorbed on the mercury electrodes in detectable amounts from millimolar solutions.

Electrochemical Generation of Isocyano Complexes from

$\text{Cr}(\text{CN})_3$. -- The voltammetry of $\text{Cr}(\text{CN})_3$ solutions containing mercury(II) or silver(I) is very similar to that just described for $\text{Cr}(\text{CN})_2^+$: Addition of mercury(II) (1.8 mmole per mmole of $\text{Cr}(\text{CN})_3$) causes the original $\text{Cr}(\text{CN})_3$ reduction wave to disappear within 5 minutes at 25°C followed by a more gradual development of new reduction waves (Figure 11). The wave that develops at the most positive potential (wave C in Figure 11) overlaps with the reduction wave for the mercury(II) adduct itself which causes it to be somewhat less distinct. The peak potentials of the three new waves that develop differ from those obtained in solutions of CrCN^{2+} or $\text{Cr}(\text{CN})_2^+$ and display different pH dependences. They appear to correspond to three different new complexes, presumably $(\text{NC})_2\text{CrNC}$, $\text{NCCr}(\text{NC})_2$ and $\text{Cr}(\text{NC})_3$ in the order of increasingly positive peak

Figure 11. -- Voltammograms of:

1 -- 1 mM Cr(CN)₃ + 1.8 mM Hg²⁺; 2 -- as in 1, 10 min after mixing; 3 -- as in 1, 20 min after mixing--no further changes occur; 4 -- 1 mM Cr(CN)₃ + 1 mM Ag¹⁺, 10 min after mixing. Supporting electrolyte was 0.1 M HClO₄-0.9 M NaClO₄; T = 22°C.



potentials. As was true with the mercury(II) adduct of $\text{Cr}(\text{CN})_2^+$, significant aquation of the tricyano complex takes place after ca. 30 minutes exposure to mercury(II). At this point waves with peak potentials matching those obtained with solutions of $\text{Cr}(\text{CN})_2^+$ and CrCN^{2+} begin to appear.

The silver(I) adducts of $\text{Cr}(\text{CN})_3$ are formed more rapidly than the Hg(II) adducts and two new reduction waves with the same peak potentials as those obtained with Hg(II) result (Figure 11, curve 4). The voltammetric data thus indicate that the same three species are generated by electroreduction of the mercury(II) and silver(I) adducts.

Potentiometric titration of solutions of $\text{Cr}(\text{CN})_3$ with Ag^+ could be completed before significant aquation occurred. A typical titration curve is shown in Figure 10, curve 2. The inflection point appears at a mole ratio of 0.64 Cr(III) per Ag(I).

Chronocoulometry could not be used to measure any adsorption of the complexes generated from the heavy metal adducts of $\text{Cr}(\text{CN})_3$ because the various waves were too poorly separated. However, electrocapillary measurements indicated no adsorption of any of the isocyano species on mercury electrodes.

Discussion

The voltammetric and titrimetric data (Figures 1-4) leave little doubt that the same species, CrNC^{2+} , that results from the reaction between Cr^{2+} and $\text{Co}(\text{NH}_3)_5\text{CN}^{2+}$ is also generated by electro-reduction of the mercury(II) and silver(I) adducts of CrCN^{2+} . The existence of both the binuclear and trinuclear adducts, $\text{MCN}(\text{Cr})$ and $\text{M}(\text{CN}(\text{Cr}))_2$ seems clearly established (Figure 3).

The values of the equilibrium quotients obtained from the potentiometric titration data were summarized in Table II. The fact that the equilibrium quotients for reactions (I) and (II) and for (III) and (IV) are not very different emphasizes the minor influence of coulombic repulsion on the stability of the adducts. The rather surprising stabilities of the adducts despite their high charges seems best understood in terms of the natural affinity of the carbon end of the cyanide ligand for the very soft cations, Ag^+ and Hg^{2+} .^{2, 3} The equilibrium quotients for reactions (II) and (IV) in Table II show $(\text{CrNC})_2\text{Ag}^{5+}$ to be less stable than $(\text{CrNC})_2\text{Hg}^{6+}$. The difference in stability is also reflected in the spectra and relative aquation rates of the two adducts. The more stable Hg^{2+} -adduct aquates more rapidly because of its weaker Cr(III)-nitrogen bond² and, correspondingly, its d-d absorption band appears at a longer wavelength ($\lambda_{\text{max}} = 565 \text{ nm}$ and 556 nm for the binuclear Hg^{2+} - and Ag^+ -adducts, respectively).

The failure of any of the isocyano chromium(III) complexes to adsorb on mercury was surprising to us. The analogous thiocyanato complexes are strongly adsorbed⁴ and in most other respects there is considerable similarity in the homogeneous coordination chemistry displayed by both sets of chromium complexes in their binding to mercury(II). To understand a possible basis for the differences in the adsorptive properties of the isocyano and thiocyanato complexes the data collected in Table IV are useful. The first point to note is that attachment of Cr^{3+} to HgCN^+ destabilizes the mercury-cyanide bond much more than the mercury-sulfur bond is destabilized when Cr^{3+} is attached to HgSCN^+ . This difference has been attributed² to a greater decrease in the σ -donating ability of the carbon end of cyanide than of the sulfur end of thiocyanate when chromium(III) is attached to the remote end of the ligand.

The adsorption data in Table IV show that uncoordinated thiocyanate ions are adsorbed much more strongly on both neutral and positively charged mercury surfaces than are cyanide ions. Thus, in adsorptive binding to a mercury surface the two anions behave differently than in their coordination to mercury(II) cations. The same reversal in the order of binding strengths also obtains (Table IV) for iodide, bromide, and azide ions compared with cyanide ion. The origin of the difference presumably lies in the very stable mercury-carbon σ -bond that is formed when Hg(II) and cyanide combine in homogeneous solution. The analogous bond on the mercury surface must be much less stable because the 6s orbital on

TABLE IV
COMPARISONS OF ION BINDING TO MERCURY(II) AND
MERCURY ELECTRODES



X^m	$\frac{[\text{HgX}^{2+m}]}{[\text{Hg}^{2+}][\text{X}^m]}$	Refer- ence	$\Gamma,^a$ moles/cm ² × 10 ¹¹		Refer- ence
			$q^m = 0$	$q^m = +10$	
CN^-	1×10^{18}	d	4.5	10	j
I^-	7.4×10^{12}	e	12	26	k
NCS^-	1.2×10^9	f	10	21	l
Br^-	1.1×10^9	e	7.2	19	m
N_3^-	3×10^7	g	5.2	16	n
Cl^-	5.5×10^6	e	2.8	13	o
CNCr^{2+}	6.5×10^{10}	h	0 ^b	0 ^b	h
SCNCr^{2+}	1.6×10^4	i	1.0 ^c	1.3 ^c	p

^a For 0.1 M solutions of the anion; q^m is the value of the electronic charge on the mercury surface in $\mu\text{C}/\text{cm}^2$. ^b For 1 mM solutions of the adsorbent. ^c For 0.5 mM solutions of the adsorbent. ^d G. Anderegg, *Helv. Chim. Acta*, **40**, 1022 (1957). ^e Reference 15. ^f L. Ciavatta and M. Grimaldi, *Inorg. Chim. Acta*, **4**, 312 (1970). ^g T. R. Musgrave and R. N. Keller, *Inorg. Chem.*, **4**, 1793 (1965). ^h This work. ⁱ Reference 3. ^j H. Wroblowa, Z. Kovac and J. O'M. Bockris, *Trans. Faraday Soc.*, **61**, 1523 (1965). ^k D. C. Grahame, *J. Amer. Chem. Soc.*, **80**, 4201 (1958). ^l R. Parsons and D. C. Symons, *Trans. Faraday Soc.*, **64**, 1077 (1968).

Table IV (Cont'd)

^mJ. Lawrence, R. Parsons and R. Payne, *J. Electroanal. Chem.*, 16, 193 (1968). ⁿC. V. D'Alkaine, E. R. Gonzalez and R. Parsons, *ibid.*, 32, 57 (1971). ^oD. C. Grahame and R. Parsons, *J. Amer. Chem. Soc.*, 83, 1291 (1961). ^pReference 4.

mercury remains essentially filled even at high positive surface charge densities (at a surface charge of $+10 \mu\text{C}/\text{cm}^2$ the average charge per mercury atom on the surface is only ca. 0.06) which makes it difficult for the cyanide ion to approach the surface atoms as closely as is required for the formation of the very stable mercury-carbon bond. The large sulfur atom in thiocyanate leads to a mercury-sulfur bond length in $\text{Hg}(\text{SCN})_4^{2-}$ of 2.5 \AA ¹⁸ which is considerably longer than the 2.0 \AA mercury-carbon bond in $\text{Hg}(\text{CN})_2$ ¹⁹ so that the presence of the filled 6s orbital in the mercury surface should produce less destabilization of the mercury-sulfur bond than it does of the mercury carbon bond in the case of cyanide.

The explanation for the nonadsorption of CrNC^{2+} to which this line of reasoning leads is then the following: The attachment of Cr(III) to cyanide produces a great decrease in the mercury-carbon bond strength in HgCNCr^{4+} . The same effect, acting on the already weaker mercury-carbon bond in adsorbed cyanide leads to a bond strength so weak that the adsorption drops below the level of detectability. Thus, the two adsorption-inhibiting factors, namely the presence of the electrons in the essentially anti-bonding 6s orbital of mercury(0) and

the partial withdrawal by the attached chromium(III) of the electron pair on cyanide that are used in forming the σ bond to mercury, combine to prevent the adsorption. The same two obstacles to adsorption are also faced by CrNCS^{2+} but the larger ligand more easily accommodates the presence of the 6s electrons and the (presumed) weakening of the chromium-nitrogen σ -bond produced by attachment to the mercury surface is partially compensated by an increased metal-to-ligand π bonding indicated by the bathochromic shift in the d-d absorption band when Hg^{2+} attaches to CrNCS^{2+} .³ The corresponding bond in CrNC^{2+} shifts to higher wave lengths upon attachment of Hg^{2+} (from < 535 nm to 565 nm) indicating a loss instead of a gain in ligand field stabilization energy. Assuming that a shift in the same direction would result from adsorption on a positively charged mercury surface, this factor would also act to decrease the tendency for CrNC^{2+} to adsorb.

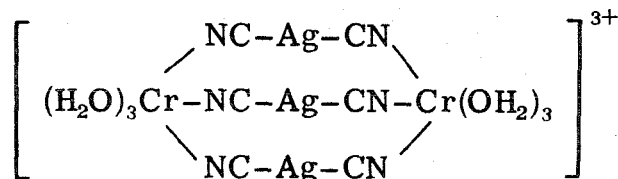
Multiple Linkage Isomers. -- The electrochemical behavior of the products obtained upon reduction of the heavy metal adducts of cis- $\text{Cr}(\text{CN})_2^+$ and fac- $\text{Cr}(\text{CN})_3$ (Figures 8, 9, 11) is consistent with the linkage isomerization of one, two or three of the cyano groups depending upon the ratio of heavy metal to complex and the time elapsed after the addition of the heavy metal. In the case of cis- $\text{Cr}(\text{CN})_2^+$ the strong implication is that both NCCrNCM and

$$\text{Cr} \begin{array}{l} \text{NC} \\ \diagdown \\ \text{M} \\ \diagup \\ \text{NC} \end{array} \quad (\text{M} = \text{Ag}^+ \text{ or } \text{Hg}^{2+})$$

are formed and, when reduced, yield NCCrNC^+ and $\text{Cr}(\text{NC})_2^+$, respectively. (A similar complex,

cis-Cr $\begin{array}{l} \text{Cl} \\ \diagdown \\ \text{Hg}^{3+} \\ \diagup \\ \text{Cl} \end{array}$, has been proposed as an intermediate in the mercury(II)-catalyzed aquation of $\text{Cr}(\text{Cl})_2^+$.²⁰⁾

Spectral evidence can be marshaled to support the conclusion that a species containing three isocyano groups results when Ag^+ is added to fac- $\text{Cr}(\text{CN})_3$ solutions in a ratio of 1.5 moles of Ag^+ per mole Cr(III) or greater: Table V gives absorption maxima for d-d bands in several complexes and values of $10 Dq$ that are calculated from the spectra and assigned to the respective ligands. These value of ligand $10 Dq$ values are used in Table V to calculate the expected positions of band maxima for heavy metal adducts containing the possible combinations of cyano and isocyano groups. The experimental spectra are included for comparison and the agreement between the calculated and experimental values is best for the fully linkage isomerized cases. The spectra of mixtures of $\text{Cr}(\text{CN})_3$ and Ag^+ become constant when the molar ratio of Ag(I) to $\text{Cr}(\text{CN})_3$ is three-to two or greater. The corresponding potentiometric titration (Figure 10) shows an inflection at this same ratio. These observations indicate the presence of a rather stable adduct having the stoichiometry $\text{Ag}_3[\text{Cr}(\text{CN})_3]_2$ and a symmetrical structure such as



suggests itself.

TABLE V
CALCULATED^a VALUES OF 10 Dq FOR THE LIGANDS
AgCN AND H₂O ON Cr(III)
d-d BAND MAXIMA

Complex	λ_{\max} , nm	10 Dq cm ⁻¹ observed	Calculated ^b
Cr(H ₂ O) ₆ ³⁺	575	17391	
Cr(H ₂ O) ₅ CN ²⁺	525	19048	(H ₂ O = 17391) CN = 27327
Cr(H ₂ O) ₅ NCAg ³⁺	556	17986	NCAg = 20961 (H ₂ O = 17391)

Comparison of observed d-d band maxima for the
Ag(I)-adducts of Cr(CN)₂⁺ and Cr(CN)₃ with those
calculated from the values of 10 Dq listed above

Mixture millimoles/l	λ_{\max} , obs nm	Possible isomer present	λ_{\max} , calc nm
2 Cr(H ₂ O) ₃ (CN) ₃ + 3 Ag ⁺	527	Cr(H ₂ O) ₃ (CN) ₂ (NCAg) ⁺	475 ^c
		Cr(H ₂ O) ₃ (CN)(NCAg) ₂ ²⁺	497 ^c
		Cr(H ₂ O) ₃ (NCAg) ₃ ³⁺	522 ^c
Cr(H ₂ O) ₄ (CN) ₂ ⁺ + Ag ⁺	540	Cr(H ₂ O) ₄ (CN)(NCAg) ²⁺	513 ^c
		Cr(H ₂ O) ₄ (NCAg) ₂ ³⁺	538 ^c

^a According to procedure outlined in reference 21.

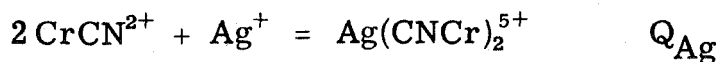
$${}^b (10 \text{ Dq})_{\text{calc}} = 6(10 \text{ Dq})_{\text{obs}} - (5 \times 17391). \quad {}^c \frac{1}{(\lambda_{\max})_{\text{calc}}} =$$

$$(10 \text{ Dq})_{\text{calc}} = \frac{17391x + 27327y + (6-x-y) 20961}{6} \quad \text{where } x \text{ and } y \text{ are}$$

the number of aquo and cyano groups, respectively, in the isomer.

Appendix

The derivation of the formulas used to evaluate the equilibrium quotients will be given for the case of silver ion only because the treatment for mercury(II) is identical. During the early stages of the titration of solutions of CrCN^{2+} with Ag^+ (or Hg^{2+}) the concentrations of the heavy metal cation is controlled by the equilibrium:



The value of $[\text{Ag}^+]$ was evaluated from equation A1:

$$[\text{Ag}^+] = 10^{\left(\frac{E_{\text{Ag}} - 0.543}{0.059} \right)} = \Theta \quad (\text{A1})$$

where E_{Ag} is the equilibrium potential assumed by the silver electrode, and 0.543 v is the experimentally observed formal potential of the Ag^+/Ag couple in the 1 M NaClO_4 -0.1 M HClO_4 supporting electrolyte employed (the corresponding value for the Hg^{2+}/Hg couple is 0.525 v).

The equilibrium concentrations of $\text{Ag}(\text{CNCr})_2^{5+}$ at each point in the titration were evaluated from the known analytical concentrations of CrCN^{2+} and Ag^+ :

$$[\text{Ag}(\text{CNCr})_2]^{5+} = C_{\text{Ag}}^0 - [\text{Ag}^+] \quad (\text{A2})$$

where C_{Ag}^0 is the total (analytical) concentration of silver present.

The equilibrium concentration of CrCN^{2+} was calculated from:

$$[\text{CrCN}^{2+}] = C_{\text{Cr}}^0 - 2[\text{Ag}(\text{CNCr})_2]^{5+} \quad (\text{A3})$$

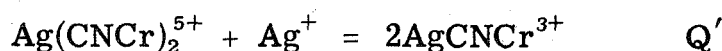
where C_{Cr}^0 is the total (analytical) concentration of CrCN^{2+} initially present.

The numerical value of Q_{Ag} was calculated from equation A4

$$Q_{\text{Ag}} = \frac{C_{\text{Ag}}^0 - \Theta}{\Theta (C_{\text{Cr}}^0 - 2C_{\text{Ag}}^0 + 2\Theta)^2} \quad (\text{A4})$$

A typical set of data for the Ag^+ -adduct is shown in the table.

When the potentiometric titrations are carried well beyond the equivalence point for formation of the trinuclear complexes the following equilibrium becomes important:



Equation A1 continues to apply and the excess of silver present assures that the concentration of CrCN^{2+} will be negligibly small so the concentrations of the trinuclear and binuclear complexes are given by

$$[\text{AgCNCr}^{3+}] = 2(C_{\text{Ag}}^0 - \frac{1}{2}C_{\text{Cr}}^0 - \Theta) \quad (\text{A5})$$

and

$$[\text{Ag}(\text{CNCr})_2]^{5+} = (C_{\text{Cr}}^0 - C_{\text{Ag}}^0 + \Theta) \quad (\text{A6})$$

Q' was therefore evaluated from equation A7.

$$Q' = \frac{4(C_{Ag} - \frac{1}{2}C_{Cr} - \Theta)^2}{\Theta(C_{Cr}^0 - C_{Ag}^0 + \Theta)} \quad (A7)$$

A typical set of data are shown in the table.

Finally, the values of Q_{III} and Q_{IV} in Table II were calculated from the experimentally measured values of Q_{Ag} and Q' according to the relations given by equations A8 and A9:

$$Q_{III} = (Q' Q_{Ag})^{\frac{1}{2}} \quad (A8)$$

$$Q_{IV} = \left(\frac{Q_{Ag}}{Q'} \right)^{\frac{1}{2}} \quad (A9)$$

POTENTIOMETRIC TITRATION OF 4.41 mM CrCN^{2+}
 (in 1 M NaClO_4 -0.1 M HClO_4) WITH 0.030 M Ag^+

C_{Cr}^0 mM	C_{Ag}^0 mM	E, mV vs. SCE	Θ $\times 10^9$	Q_{Ag} $\times 10^{10}$
4.34	0.472	41	2.71	1.5
4.30	0.703	44	3.05	2.8
4.26	0.93	50	3.06	4.2
4.23	1.15	60	5.72	5.4
4.20	1.37	73	9.53	6.7
4.17	1.59	91	19.3	8.4
4.14	1.80	132	96.9	6.4

Average = 5.1

			$\Theta \times 10^4$	Q'
4.01	2.63	322	1.69	3.2
3.99	2.83	334	2.71	3.3
3.96	3.02	342	3.72	3.7
3.93	3.21	349	4.89	3.9
3.87	3.59	360	7.54	4.2
3.85	3.78	364	8.82	4.5

Average = 3.9

References

1. J. P. Birk and J. H. Espenson, Inorg. Chem., 7, 991 (1968).
2. J. H. Espenson and W. R. Bushey, ibid., 10, 2457 (1971).
3. J. N. Armor and A. Haim, J. Amer. Chem. Soc., 93, 867 (1971).
4. D. J. Barclay, E. Passeron, and F. C. Anson, Inorg. Chem., 9, 1024 (1970).
5. D. I. Bustin and J. E. Earley, ibid., 7, 1238 (1968).
6. H. Siebert, Z. anorg. allgem. Chem., 327, 63 (1964).
7. A. Haim and W. K. Wilmarth, J. Amer. Chem. Soc., 83, 509 (1961).
8. W. B. Schaap, R. Krishnamurthy, D. K. Wakefield, and W. F. Coleman, "Coordination Chemistry", S. Kirschner, Editor, Plenum Press, New York, N. Y., 1967, p. 117.
9. G. W. Haupt, J. Res. Nat. Bur. Stand., 48, 414 (1952).
10. F. C. Anson, Anal. Chem., 38, 54 (1966).
11. J. P. Birk and J. H. Espenson, J. Amer. Chem. Soc., 90, 1153 (1968).
12. An earlier, unsuccessful attempt to observe CrNC^{2+} polarographically⁵ was performed at a higher temperature, 15°C, where the half-life of CrNC^{2+} would have been less than 70 seconds.¹¹
13. J. J. Ulrich and F. C. Anson, Inorg. Chem., 8, 195 (1969).
14. R. S. Nicholson and I. Shain, Anal. Chem., 36, 706 (1964).

15. L. G. Sillén and A. E. Martell, "Stability Constants of Metal-Ion Complexes", Chemical Society London, 1964.
16. J. P. Birk and J. H. Espenson, J. Amer. Chem. Soc., 90, 2266 (1968).
17. The charge-time behavior on stepping the electrode potential to the diffusion limited plateau of Hg(II) is given by the usual chronocoulometric relationship¹⁰

$$Q_{\text{Hg}} = 2nFA(D_{\text{Hg}}/\pi)^{1/2} C_{\text{Hg}}^0 t^{1/2} + \text{Intercept}_{\text{Hg}}$$

On stepping the potential at $t = \tau$ to the diffusion limited region of Cr(III) with the condition that $(D_{\text{Cr}})^{1/2} C_{\text{Cr}}^0$ is effectively equal to $2(D_{\text{Hg}})^{1/2} C_{\text{Hg}}^0$

$$Q_{\text{Total}} = Q_{\text{Hg}} + 4nFA(D_{\text{Hg}}/\pi)^{1/2} C_{\text{Hg}}^0 (t - \tau)^{1/2} + \text{Intercept}_{\text{Cr}}$$

The charge due only to chromium reduction is then

$$Q_{\text{Cr}} = Q - Q_{\text{Hg}} = 4nFA(D_{\text{Hg}}/\pi)^{1/2} C_{\text{Hg}}^0 (t - \tau)^{1/2} + \text{Intercept}_{\text{Cr}}$$

$$\text{with } \text{Intercept}_{\text{Cr}} = Q_{dl} + nF\Gamma_{\text{Cr}}$$

18. H. Scouloudi, Acta Crystallogr., 6, 651 (1953).
19. A. F. Wells, Structural Inorganic Chemistry, 3rd Ed., Oxford Press, London, 1962, p. 892.
20. J. P. Birk, Inorg. Chem., 9, 735 (1970).
21. B. N. Figgis, Introduction to Ligand Fields, Interscience Publishers, New York, N. Y., 1966, p. 236.

Part II

Adsorption of Azido- and Isothiocyanatochromium(III) and
Azidocobalt(III) Complexes on Mercury Electrodes

The substitutional inertness of certain transition-metal ions would seem to make them ideal systems for studies of adsorption of metal ions on electrodes. The known identity of the adsorbing species coupled with large number of possible complexes contrasts favorably with similar studies of the anion induced adsorption of white metal cations (d^{10} systems)¹ where the lability of the complexes complicates the determination of the adsorption mechanism. A necessary, although not always sufficient, criterion for adsorption of a metal complex is the presence of an ambidental ligand capable of simultaneous bonding to the metal cation and the electrode surface. For mercury electrodes, ions or neutral molecules that spontaneously adsorb from solution would be logical choices for such ligands. Although bromide and iodide ions fall into such a category, the monofunctional nature of these ions make it unlikely that they would be sufficiently good nucleophiles when complexed to a transition-metal cation to induce significant adsorption. Ions such as cyanide and thiocyanate which bond to mercury via carbon or sulfur and are capable of bonding to the transition metal through nitrogen^{2, 3} are better choices as ligands.

However, a recent study of several isocyanochromium(III) complexes⁴ showed them not to be adsorbed. Reasons for their non-adsorption were advanced.

Tanaka et al.⁵ have studied the adsorption of a number of chromium(III) thiocyanate complexes on mercury electrodes using electrocapillary techniques. The amount of adsorption was found to

be dependent on the number and configuration of coordinated thiocyanates as well as on the nature of the other coordinated ligands. More recently, the adsorption of a number of other transition-metal thiocyanates has been measured.^{6, 7} These investigations led to the observation that a correlation may exist between the net ligand field stabilization energy (LFSE) of an isothiocyanato complex and the amount of its adsorption. The proposed rationalization for this observation was that bonding of the complex to the electrode by means of the exposed sulfur atom in a coordinated isothiocyanate complex increases its LFSE (possibly in a manner proportional to the original LFSE) which thereby provides the driving force for adsorption.

The present research was initiated in order to explore the factors affecting the adsorption of transition-metal thiocyanates, in particular, the LFSE aspect, and to see if similar behavior is displayed by other complexes. Reported here are adsorption measurements of a number of azidocobalt(III) and azido- and isothiocyanatochromium(III) complexes.

Experimental Section

Materials. -- Commercially available chemicals of reagent grade quality were used without further purification unless otherwise noted.

For the majority of ammine and ethylenediamine complexes, synthesis consisted of heating an aqueous solution of the appropriate starting complex with an excess of azide or thiocyanate salt. The desired compound either crystallized on cooling or was precipitated by addition of a large excess of anion. The resulting complexes were usually converted to the corresponding perchlorate salts by dissolving in the minimum amount of warm H₂O and adding a small excess of NaClO₄. The products were then recrystallized from warm H₂O and stored in the dark to prevent photocatalyzed decomposition.

Isothiocyanatopentaamminechromium(III) perchlorate⁸ was prepared from aquopentaamminechromium(III) ammonium nitrate.⁹ Repeated recrystallizations from warm H₂O were required before a compound of sufficient purity was obtained.

Chloroaquotetraamminechromium(III) chloride,¹⁰ prepared from oxalatotetraamminechromium(III) nitrate,¹⁰ was used as the starting product for the synthesis of cis-diisothiocyanatotetraamminechromium(III) perchlorate.¹¹

Cis-diisothiocyanatobis(ethylenediamine)chromium(III) perchlorate was prepared according to Pfeiffer¹² from cis-dichlorobis(ethylenediamine)chromium(III) chloride.¹³

Trans-diisothiocyanatobis(ethylenediamine)chromium(III) was prepared as described in the literature¹³ and converted to the perchlorate.

Cis-diazidobis(ethylenediamine)cobalt nitrate was synthesized by the methods described by Staples and Tobe.¹⁴ Both methods, one employing trans-dichlorobis(ethylenediamine)cobalt(III) chloride,¹⁵ and the other using cobalt(II) and ethylenediamine were used for the synthesis. No differences in electrochemical properties could be detected between the complexes prepared by either of the above methods. The filtrate from the former preparation was used to obtain the trans isomer¹⁴ as the perchlorate. The cis complex was used as the nitrate salt.

The preparation of cis-diazidobis(ethylenediamine)chromium-(III) perchlorate followed closely the procedure of Linhard and Weigel.¹⁶

Azidopentaamminechromium(III) perchlorate was prepared as described¹⁷ from aquopentaamminechromium(III) perchlorate.

Cis-diazidotetraaquo chromium(III) perchlorate was synthesized by a modification of the method of Snellgrove and King.¹⁸ In a typical preparation, 20 ml of 0.08 M Cr^{+2} , prepared electrolytically from $\text{Cr}(\text{ClO}_4)_3$, was added to an oxygen-free solution 0.4 M in both NaN_3 and HN_3 . The +1 species were separated from other species on a cation exchange column, Bio-Rad AG 50W-X4, 100-200 mesh in the sodium form purified as described previously.⁵ The solution was then acidified and the excess azide removed as volatile HN_3 by bubbling

the solution with nitrogen. Cr^{+2} was then added to convert the trans isomer to the monoazido complex and another separation carried out on the column. Both purity and concentration were determined by comparing the absorbancy at $275 \text{ m}\mu$ ($\epsilon = 5900$)¹⁹ with that expected from a chromium determination.²⁰

Potassium hexathiocyanatochromium(III), $\text{K}_3\text{Cr}(\text{NCS})_6 \cdot 4 \text{H}_2\text{O}$ (Alpha Inorganics) and Reinecke Salt, trans- $\text{NH}_4[\text{Cr}(\text{NCS})_4(\text{NH}_3)_2]$ · H_2O (Baker), were recrystallized from H_2O at room temperature on a roto-evaporator.

The complexes were characterized by their respective spectra. In some cases, a considerable variation in spectral properties has been reported.²¹ In these instances a chromium analysis²⁰ was performed and a comparison made with the chromium content expected from the assumed molecular weight.

Due to the insolubility of many of the complexes in a perchlorate medium, most electrochemical experiments were carried out in a sodium sulfate-bisulfate buffer of ionic strength 1 (0.32 M Na_2SO_4 and 0.03 M NaHSO_4 , pH ~ 2.2). Where NaClO_4 was used as a supporting electrolyte, its concentration was always 1 M. The sodium perchlorate was prepared as described previously.⁴ All solutions were prepared from triply distilled water and deaerated with prepurified nitrogen. The temperature was constant at $23 \pm 2^\circ$.

Apparatus. -- The instrumental apparatus for linear potential sweep voltammetry and chronocoulometry is similar to that described previously.⁷ Potentials were measured with respect to

NaCl-saturated calomel electrode but are reported vs. the KCl-saturated calomel electrode (SCE). Controlled potential electrolysis at a mercury pool was performed with a Wenking Potentiostat (Model TR) following standard procedures.²²

A two compartment cell that isolated the reference electrode from the main compartment by a glass frit was employed in the potential sweep and chronocoulometric experiments. A commercially available hanging mercury drop electrode (HMDE) (Brinkman Instruments, Inc.) was used as the working electrode and a platinum wire served as the auxiliary electrode. The working electrode area was 0.032 cm². All potential sweep experiments were recorded at 10 V/sec on a Tektronix Model 564 storage oscilloscope.

Spectra were recorded with a Cary 11 spectrophotometer or by means of a manual Beckman DU spectrophotometer equipped with Gilford Absorbance Indicator, Model 220.

Electrochemical Procedures. -- Owing to the chemical irreversibility of all the electrochemical reactions investigated conventional double potential-step chronocoulometry²³ could not be used to measure reactant adsorption. Instead, the working electrode was connected at an initial potential, E_i , where no reactions occur for sufficient time to obtain adsorption equilibrium. The potential was then stepped to a final potential, E_f , sufficiently negative for reduction of the complex to occur at a diffusion limited rate and a standard least-squares analysis of the resulting charge-time data performed.²³ In a typical experiment, 100 data points at 400 μ sec

intervals were taken. The intercept obtained from the least-squares analysis gives $F\Gamma + Q_{dl}$ where F is Faraday's constant, Γ , the adsorption in moles/cm² and Q_{dl} , the double-layer charge change that occurs on stepping the potential from E_i to E_f . Q_{dl} was determined for some solutions by measuring the charge that flows into a dropping mercury electrode (DME) in contact with the solution of interest at E_i . The charge at E_f was determined for the supporting electrolyte with no electroactive species present. Since no evidence was found for product adsorption, the charge at E_f should be the same in both in the presence and absence of the adsorbing compound. Q_{dl} is simply the difference between the two charges.

The charge-time behavior obtained with the DME at E_i was analyzed according to Lauer and Osteryoung.²⁴ Data were taken every 0.01 sec utilizing a data acquisition system similar to that for chronocoulometry and the analysis performed over 0.5 to 1.5 sec of drop life.

The DME method is useful for measuring electrode charge, Q_m , for solution concentrations down to approximately 0.2 mM if the analysis is performed at later stages of drop development. For solutions less concentrated than this, however, adsorption equilibrium can not be obtained during the life of the drop. Fortunately, in most cases, the charge at one or more potentials did not depend significantly on the concentration of the adsorbing compound. In these cases, the charge at any potential anodic of complex reduction could be obtained by the stepping the potential of the hanging drop electrode from E_i , where Q_m is known to E_f , where Q_m is to be determined.

The intercept of a $Q - t^{1/2}$ plot gives the Q_{dl} for the potential step from which Q_m at E_f can be evaluated. This method could possibly lead to some error in the determination of Q_m since adsorption equilibrium is probably not reached instantaneously at E_f . However, a test of this technique in more concentrated solutions where Q_m is known from DME measurements reproduced the Q_m values to better than $\pm 1 \mu\text{C}/\text{cm}^2$.

A combination of the DME and potential step methods was used to evaluate the Q_m values for a series of solution concentrations selected such that Q_m at a given potential does not vary too much in going from one solution to the next. Q_m values for solutions of intermediate concentrations were obtained by extrapolation of the data for the known solutions. An insignificant error is expected to result from the extrapolation.

In some of the more dilute solutions, times greater than 5 min were required for adsorption equilibrium to be reached. To shorten these times somewhat, a small stream of nitrogen was bubbled through the solution in a number of experiments.

Results

Electrochemistry of the Complexes. -- All of the complexes studied in the chronocoulometric experiments are reduced in a one-electron step with ultimate formation of the dipositive hexaaquo ions. Table I gives the observed peak potentials at a sweep rate of 10 V/sec and the potentials for the onset of polarographic current. Polarographic half-wave potentials are not listed in Table I because polarographic maxima present with most of the compounds made an accurate determination impossible. Experimentally it is found that E_f must be approximately 100 mv more cathodic than the voltammetric peaks in order for diffusion limited kinetics to obtain under chronocoulometric conditions. E_i must be somewhat positive of the onset of current to prevent concentration polarization at the electrode. The most positive potential for E_i was chosen to be 100 to 200 mv negative of the point at which appreciable anodic current (probably reflecting incipient reaction between the complex and electrode) was observed. This potential varied considerably from one complex to the other. In no case did the anodic limit on E_i appear to result from the presence of free azide or thiocyanate ions.

Polarograms for a number of the thiocyanate complexes have been run previously in the presence of maxima suppressor²⁵ and the half-waves reported are consistent with present results except for trans- $\text{Cr}(\text{NCS})_4(\text{NH}_3)_2^-$ where the onset of polarographic current in the present investigation is very near the reported half-wave.²⁵

TABLE I
PEAK POTENTIALS^a AND ONSET OF POLAROGRAPHIC CURRENT

Complex	E_p, V^b	Onset of current, V^b	Electrolyte
$[Cr(NH_3)_5NCS][ClO_4]_2$	-1.120	-0.80	$Na_2SO_4^c$
<u>cis</u> - $[Cr(NH_3)_4(NCS)_2][ClO_4]$	-1.096	-0.63	$Na_2SO_4^c$
<u>cis</u> - $[Cr en_2(NCS)_2][ClO_4]$	-1.040	-0.70	$Na_2SO_4^c$
<u>trans</u> - $[Cr en_2(NCS)_2][ClO_4]$	-1.078	-0.40	$Na_2SO_4^c$
<u>trans</u> - $NH_4[Cr(NCS)_4(NH_3)_2]$	-0.94, -1.00 ^d	-0.74	$Na_2SO_4^c$
$K_3Cr(NCS)_6$	-0.78	-0.40	$Na_2SO_4^c$
<u>cis</u> - $[Co en_2(N_3)_2][NO_3]$	-0.034	+0.33	$NaClO_4^e$
	-0.094	+0.25	$Na_2SO_4^c$
<u>trans</u> - $[Co en_2(N_3)_2][ClO_4]$	-0.110	+0.23	$NaClO_4^e$
	-0.168	+0.12	$Na_2SO_4^c$
<u>cis</u> - $[Cr en_2(N_3)_2][ClO_4]$	-1.122 ^f	-0.9 ^g	$NaClO_4^h$
<u>cis</u> - $[Cr(H_2O)_4(N_3)_2][ClO_4]^i$	-1.248	~ -0.65	$NaClO_4^j$
	-1.138	~ -0.55	$NaClO_4^k$
$[Cr(NH_3)_5N_3][ClO_4]_2$	-1.150		$NaClO_4^e$

TABLE I (Cont'd)

- ^a Sweep rate = 10 v/sec.
- ^b Potentials reported vs. SCE.
- ^c 0.319 M Na₂SO₄ and 0.31 M NaHSO₄, pH ~ 2.2.
- ^d Dual peak.
- ^e 1 M NaClO₄, pH variable but < 2.
- ^f pH independent.
- ^g -0.7 when pH = 2.
- ^h 1 M NaClO₄, pH ~ 5.5.
- ⁱ cis-Cr(H₂O)₄(N₃)₂ was the only complex studied with a measurable pH dependent peak potential.
- ^j 1 M NaClO₄, pH = 2.5.
- ^k 1 M NaClO₄, pH = 1.2.

Also, the maximum decays at ~1.05 to -1.2 V to a current that appears to be on the rising portion of a polarographic wave and is significantly less than the diffusion limited value. This and evidence presented later indicate that in the absence of maxima suppressor Cr(NCS)₄(NH₃)₂⁻ is self-inhibiting. Evidence for suppression was also found for Cr(NCS)₆⁻³. The polarographic limiting current did not increase commensurate with an increase in concentration in apparent disagreement with the earlier finding.²⁵ It is interesting to note that the position of the voltammetric peak is independent of concentration and with the polarographic results indicate that at least for Cr(NCS)₆⁻³

the suppression may reflect a decrease in the effective electrode area. (In a previous investigation of $\text{Cr}(\text{NCS})_6^{-3}$ ²⁶ a dip in the polarographic limiting current was observed at $\sim -0.9\text{V}$ and attributed to repulsion of the negative complex from the negatively charged electrode.

A similar dip was not observed by us but our results do not rule out a possible double-layer effect as a contributing factor in the observed behavior.) In solutions of $\text{Cr}(\text{NCS})_6^{-3}$ E_i was limited to potential negative of -0.2 due to the onset of apparent oxidative reactions at $\sim -0.17\text{V}$. Similar behavior has been previously observed.²⁶

The linear sweep voltammograms of cis and trans- $\text{Cr}(\text{en})_2(\text{NCS})_2^+$ and $\text{Cr}(\text{NCS})_6^{-3}$ are complicated by maxima at the HMDE. The maxima are a function of both sweep rate and concentration, generally decreasing with a decrease in concentration and an increase in sweep rate. Under certain conditions, two closely-spaced peaks appear in voltammograms of cis- $\text{Co}(\text{en})_2(\text{N}_3)_2^+$ and trans- $\text{Cr}(\text{NCS})_4(\text{NH}_3)_2^-$ solutions which may either result from reduction of adsorbed species or arise from maxima at the HMDE. Voltammograms of cis and trans- $\text{Co}(\text{en})_2(\text{N}_3)_2^+$ also display rather broad and quite noticeable maxima beginning at ~ -0.4 to -0.8V , far removed from the complexes reduction potentials. Polarograms of the $\text{Co}(\text{en})_2(\text{N}_3)_2^+$ complexes showed gradual increases in current in the diffusion plateau region as the potential became more negative. The potential where the increase in current begins is strongly dependent on concentration, moving positive and increasing in magnitude with an increase in concentration. $\text{Co}(\text{II})$ is known to react with organic azides²⁷ and a similar

mechanism may be operative here to generate Co(III) at the electrode giving rise to maxima of catalytic origin. A small pre-peak appears as a shoulder on the voltammetric peak for cis-Cr(NH₃)₄(NCS)₂⁺¹ and appears to be due to reduction of adsorbed complex.

All of the azido chromium(III) complexes display catalytic currents that increase with a decrease in pH. The catalytic currents for Cr(NH₃)₅N₃⁺² and cis-Cr(H₂O)₄(N₃)₂⁺ were about the same but were much less than the catalytic current for cis-Cr(en)₂(N₃)₂⁺. The homogeneous rate constant for the reaction of Cr⁺² with hydrozoic acid²⁸ combined with the high concentration of Cr⁺² in the diffuse-layer is sufficient to account for the catalytic currents for Cr(NH₃)₅N₃⁺² and cis-Cr(H₂O)₄(N₃)₂⁺ but not for cis-Cr(en)₂(N₃)₂⁺. This suggests that a chromium(II) ethylenediamine complex that reacts much more rapidly with HN₃ may be a transient product of the electrode reaction.

Adsorption of the Complexes: Cr(NH₃)₅NCS⁺² and trans-Cr(en)₂(NCS)₂⁺. -- The results of adsorption measurements for Cr(NH₃)₅NCS⁺² and trans-Cr(en)₂(NCS)₂⁺ along with previously obtained results for Cr(H₂O)₅NCS⁺² are given in Table II. The measurements for Cr(H₂O)₅NCS⁺² were carried out in NaClO₄ electrolyte whereas measurements for Cr(NH₃)₅NCS⁺² and trans-Cr(en)₂(NCS)₂⁺¹ owing to their lack of solubility in NaClO₄ were made in HSO₄⁻-SO₄⁻² electrolyte. The table shows that Cr(NH₃)₅NCS⁺² is somewhat more strongly adsorbed than Cr(H₂O)₅NCS⁺². The difference in adsorbing is probably greater than depicted here since, as is shown later, SO₄⁻² is rather strongly adsorbed itself and therefore has a tendency to decrease the

TABLE II

ADSORPTION^a OF $\text{Cr}(\text{NH}_3)_5\text{NCS}^{+2}$, $\text{trans-Cr}(\text{en})_2(\text{NCS})_2^+$ AND

$\text{Cr}(\text{H}_2\text{O})_5\text{NCS}^{+2}$ ON MERCURY ELECTRODES

Potential mV vs. SCE	$\text{Cr}(\text{H}_2\text{O})_5\text{NCS}^{+2}$ b, c		$\text{Cr}(\text{NH}_3)_5\text{NCS}^{+2}$ d		$\text{trans-Cr}(\text{en})_2(\text{NCS})_2^+$ d	
	0.5 mM	0.8 mM	0.4 mM	0.4 mM	0.8 mM	0.4 mM
0.2	0.6					
0.1	0.8	3.9	1.4		3.2	1.7
0.0	1.1	3.2	1.5		2.9	1.8
-0.1	1.3	2.8	1.4		3.0	1.4
-0.2	1.3	3.2	1.4		4.0	2.1
-0.3	1.0	3.3	1.6		5.5	3.1
-0.4	1.0	3.5	1.6		9.1	7.3
-0.5		2.7	1.1		10.3	8.7
-0.6		2.1	1.2		11.2	10.2
-0.7		1.4			11.9	11.2
					8.8	7.0

^a Adsorption = $F\Gamma$, Γ in $\mu\text{C}/\text{cm}^2$.

^b Values obtained from ref. 7.

^c Supporting electrolyte = 1 M NaClO_4 .

^d Supporting electrolyte = 0.32 M Na_2SO_4 + 0.031 M NaHSO_4 .

adsorption of weakly adsorbing species compared with the values found in less strongly adsorbing perchlorate electrolyte. At more negative potentials trans-Cr(en)₂(NCS)₂⁺ is much more strongly adsorbed than Cr(NH₃)₅NCS⁺². There appears to be little difference in the adsorption of the two complexes positive of ~ -0.2 V. This is probably due to the leveling effect of SO₄⁻² described above. Several attempts were made to measure adsorption in solutions more concentrated than 1.6 mM in trans-Cr(en)₂(NCS)₂⁺ in order to reach a maximum adsorption.

However, at concentrations greater than 1.6 mM the chronocoulometric slopes were much greater than those expected for the concentrations used and the intercepts decreased, sometimes to values below Q_{dl} .

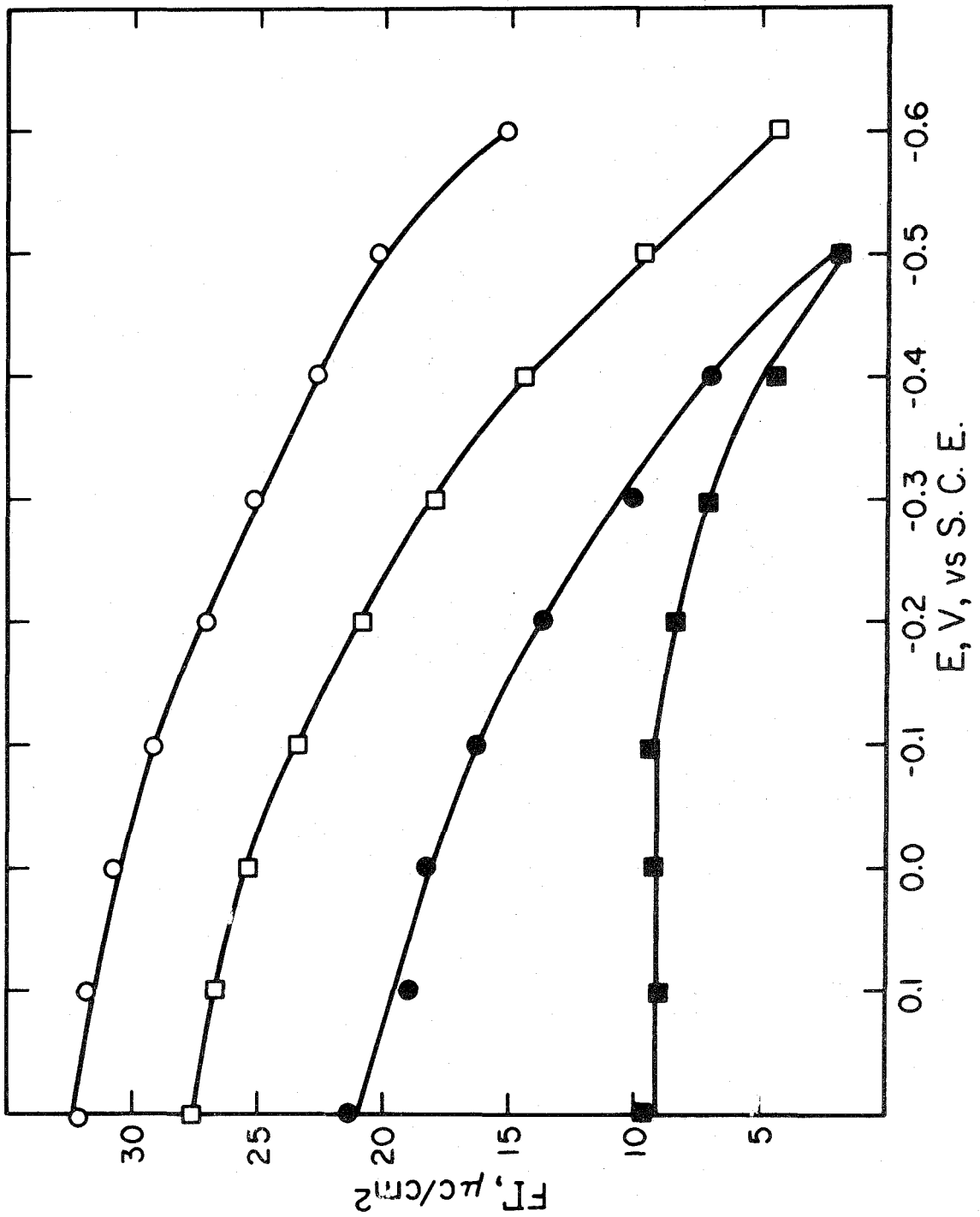
The standard deviations of the slopes also became quite large.

Similar problems were found for potentials positive of -0.4 V with the 1.6 mM solution. It is likely that these problems are associated with the maxima mentioned above, i. e., spontaneous stirring of the solution layer at the surface of the liquid metal electrode.

cis-Cr(NH₃)₄(NCS)₂⁺. -- The adsorption as a function of potential for a number of concentrations of cis-Cr(NH₃)₄(NCS)₂⁺ is shown in Figure 1. No increase in adsorption was found on increasing the concentration above 0.4 mM positive of -0.2 V. The saturation value of the adsorption thus appears to be potential dependent decreasing as the potential is made more negative. The saturation value of the adsorption, $F\Gamma$, assuming a rectangularly packed monolayer (dimensions of the rectangle were taken as the S to S distance and the trans-H₃N to H₃N distance) and using the interatomic distances for

Figure 1. -- Adsorption of cis-Cr(NH₃)₄(NCS)₂⁺
as a function of potential

○ -- 0.8 mM; □ -- 0.08 mM; ● -- 0.02 mM;
■ -- 0.01 mM. Supporting electrolyte, 0.32 M
Na₂SO₄ + 0.031 M NaHSO₄.



Reinecke salt²⁹ is calculated to be $\sim 34 \mu\text{C}/\text{cm}^2$. This is close to $33 \mu\text{C}/\text{cm}^2$ obtained experimentally at $+0.2 \text{ V}$.

The rather marked potential dependence of the adsorption led us to wonder if the complex was still adsorbed at potentials negative of -0.7 where reduction takes place. Osteryoung and Christie³⁰ have described a method for determining if complete desorption takes place using a double potential step procedure, stepping to progressively more negative (or positive) potentials, and analyzing the charge time data for the second step. If the time spent at the initial potential of the second potential step is short, i. e., on the order of a few msec so that little bulk complex is reduced, this method can be used to determine if cis- $\text{Cr}(\text{NH}_3)_4(\text{NCS})_2^+$ is desorbed negative of -0.7 V . Performing just such an experiment with a 0.08 mM solution, where the charge due to diffusing species is small, indicated that no desorption took place at -0.85 V . Even a cursory examination of Figure 1 shows that this can not be true. However, the extensive desorption resulting from stepping the potential from more positive values to -0.85 V would increase the concentration of the complex at the electrode surface to quite high values and, if there is a residual tendency for cis- $\text{Cr}(\text{NH}_3)_4(\text{NCS})_2^+$ to adsorb at -0.85 V , the high local concentration of complex could lead to its continued adsorption. The effect of such a process would be to produce an apparently slow desorption. Using higher concentrations and stepping to -0.7 V permits one to wait for longer times before commencing the second potential step. Investigation of the FT-time behavior at -0.7 V

indicated that the desorption is indeed slow. Nearly 100 msec elapse before the apparent adsorption at -0.7 V in a 0.8 mM solution decays to its equilibrium value.

The adsorption plotted vs. $\ln C$ for a number of potentials in Figure 2 shows a large increase over a fairly small concentration range. The increase in adsorption per decade increase in C is considerably larger than that for a compound obeying a Langmuir isotherm.³¹ This is depicted more graphically in Figure 3 where the adsorption is plotted on Langmuirian coordinates. The constant potential isotherm at $+0.2$ V is also at constant charge since the electrode charge is independent of adsorption positive of -0.1 V. If the assumption is made that the adsorption adheres to a Langmuir isotherm at the lowest coverages measured ($\theta < 0.05$) then the difference at constant coverage, θ , between the experimental curves and the dashed line is a measure of the difference in free energy of adsorption between an ideal Langmuirian system with only particle-electrode interactions (except for the steric forces that prevent two particles from simultaneously occupying the same adsorption site) and a nonideal system where particle-particle interactions may become important. The experimental curves lie above the line corresponding to a compound obeying Langmuirian adsorption (Figure 3). For the present system this requires that at least at some coverages the free energy of adsorption be increased by a favorable interparticle interaction.

Figure 2. -- Adsorption of cis-Cr(NH₃)₄(NCS)₂⁺ as function of $-\ln C$ (C in mole/l).

○ -- +0.2 V; □ -- 0.0 V; ● -- 0.2 V; ■ -- 0.4 V
vs. S. C. E. Supporting electrolyte, 0.32 M Na₂SO₄ + 0.031 M NaHSO₄.

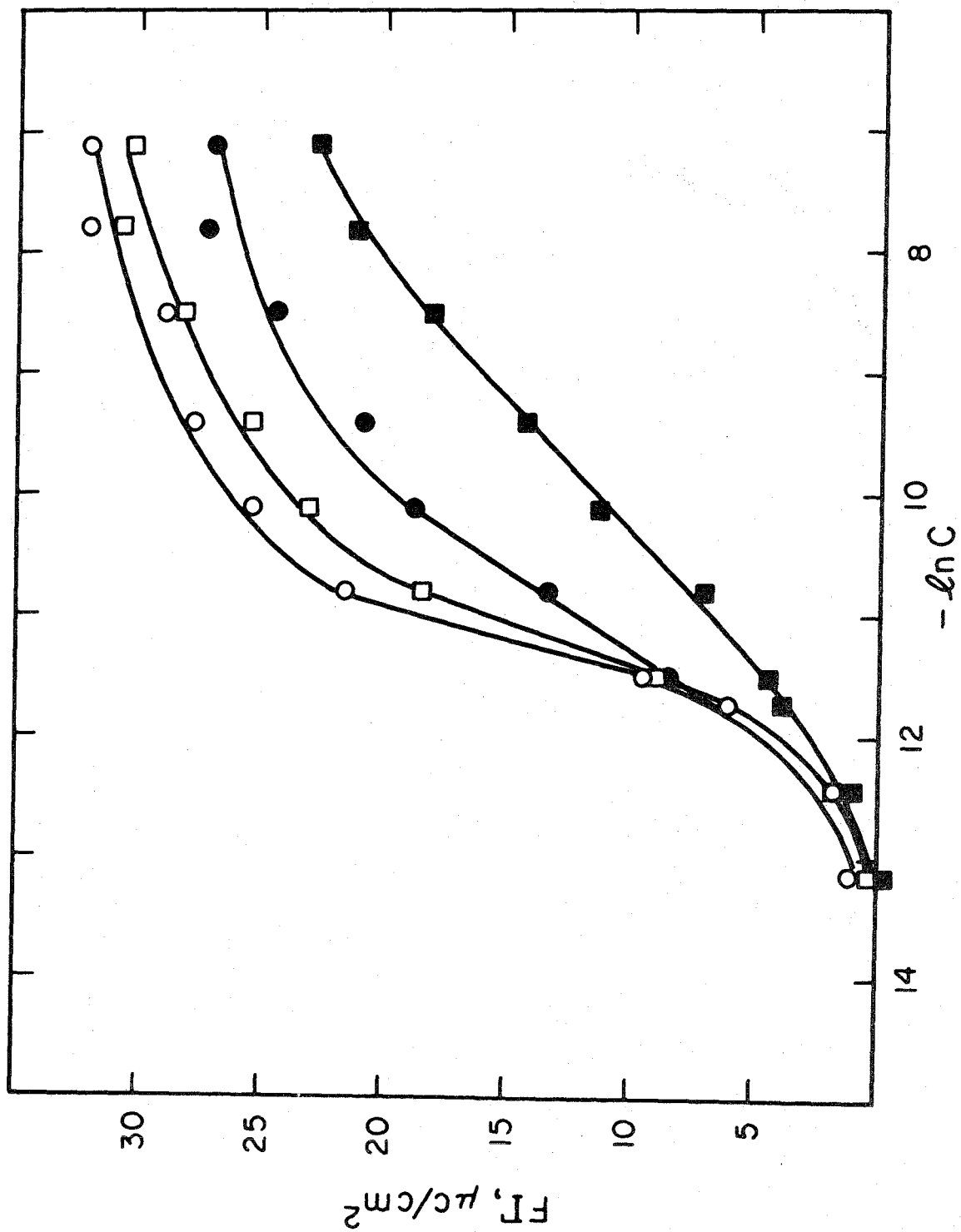
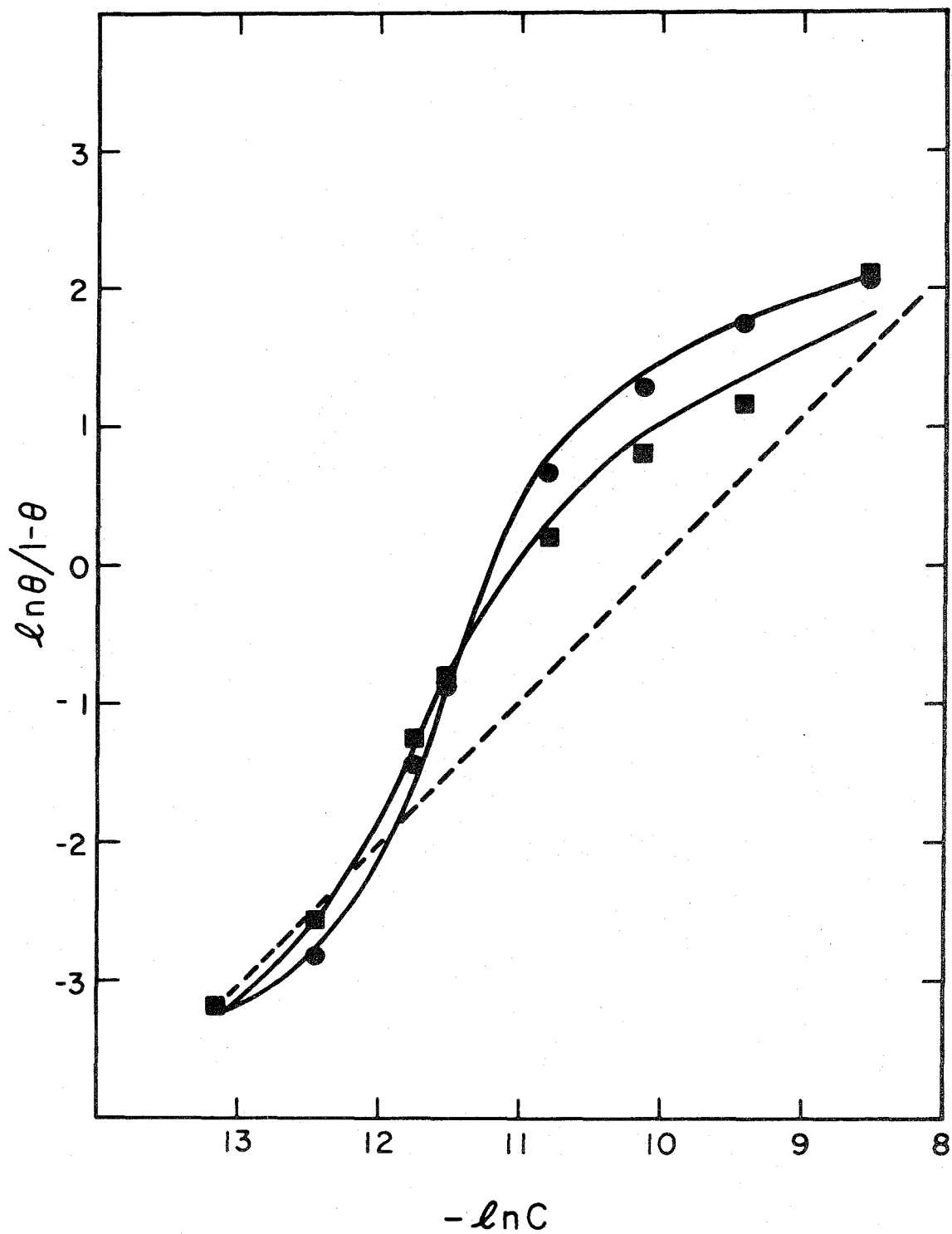


Figure 3. -- Adsorption of cis-Cr(NH₃)₄(NCS)₂⁺ plotted on Langmuirian coordinates, $\ln \frac{\theta}{1-\theta}$ vs. $-\ln C$ (C in mole/l).

● -- + 0.2 V; ■ -- -0.2 V vs. S. C. E., Dashed line is a Langmuir isotherm. Supporting electrolyte = 0.32 M Na₂SO₄ + 0.031 M NaHSO₄.



In Figure 4 the data have been fitted to a Frumkin isotherm,

$$\ln(\beta c) = \ln \frac{\theta}{1-\theta} + A\theta, \quad (1)$$

which allows for interparticle interactions. In the above $\beta = (\exp - \Delta G^0/RT)/\Gamma_s$; c , the concentration, and A is the interaction parameter. Rearrangement of (1) yields the coordinates of Figure 4 with a slope, A , and an intercept, $-\ln \beta$. Two regions are apparent in Figure 4. When $\theta < 0.8$, $A < 0$ and the predominate interaction between adsorbed molecules is attractive. For $\theta > 0.8$ the interaction becomes repulsive ($A > 0$). These two apparently contradictory results indicate that either two Frumkin isotherms are involved depending on coverage or an interaction term of the form

$$A\theta^X + B\theta^Y$$

applies. The implicit assumption of the Frumkin isotherm as expressed in equation 1 is that only one interaction or interactions that depend on coverage in the same manner contribute significantly to the A term. This assumption is not a restriction in the use of a Frumkin isotherm and one is entirely justified in considering any number of interactions of different θ dependence simultaneously. The Frumkin isotherm would then be of the form

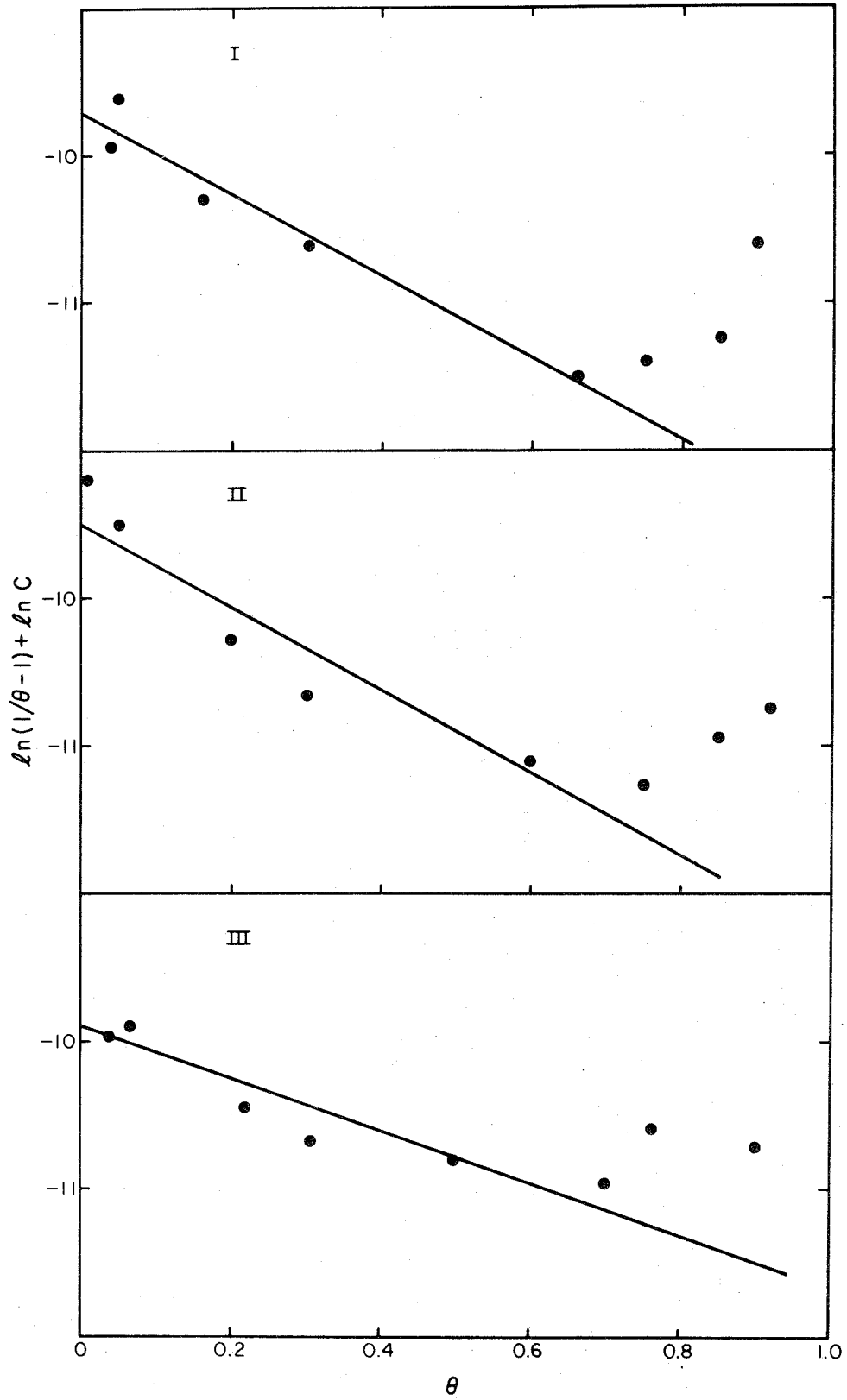
$$\ln(\beta c) = \ln \frac{\theta}{1-\theta} + A\theta^X + B\theta^Y + \dots$$

Figure 4. -- Adsorption of cis-Cr(NH₃)₄(NCS)₂⁺ fitted to a Frumkin isotherm. Rearrangement of $\ln(\beta c) = \ln\left(\frac{\theta}{1-\theta}\right) + A\theta$ yields the coordinates of the graph. The lines are a least-squares fit to the descending points with a slope, A, and an intercept, $-\ln \beta$, where $\ln \beta = -\Delta G^0/RT - \ln \Gamma_s$.

I -- +0.2 V, A = -2.8 and cept = -9.7;

II -- 0.0V, A = -2.7 and cept = -9.5;

III -- -0.2 V, A = -1.6 and cept = -9.9.

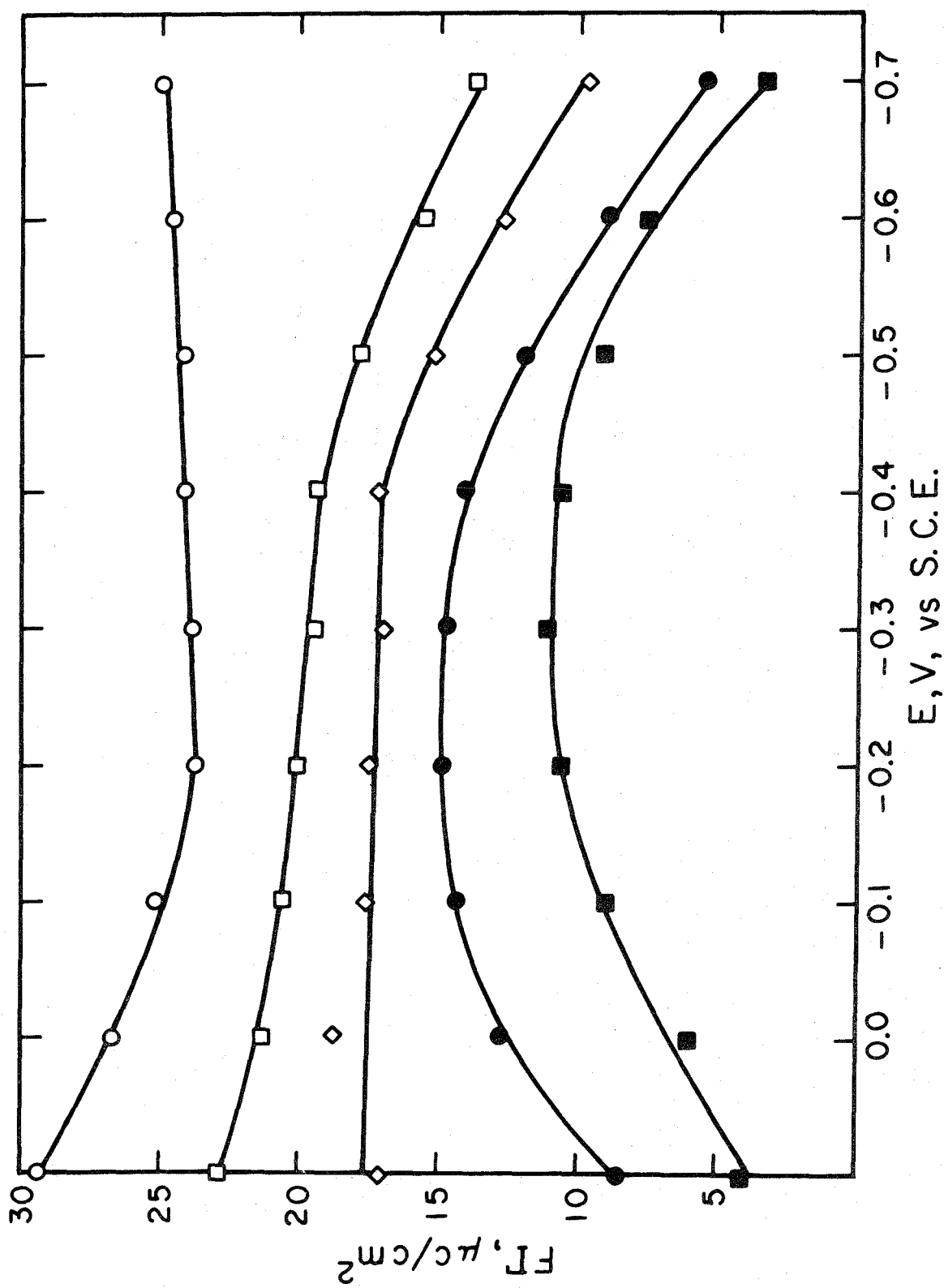


In the present case only the first two terms of the interaction are necessary to represent the results. $A\theta^X$ dominates for $\theta < 0.8$ and $B\theta^Y$ dominates for $\theta > 0.8$. Obviously then, there is no real reason to expect the data in Figure 4 to be linear in θ . This may be partly responsible for the scatter of data in Figure 4, and the slopes of the lines fit to this data can only be an approximation of the true attraction. Values for A in Figure 4 represent the range of A observed between +0.2 and -0.2 V as do the intercepts. The intercepts represent a standard free energy of adsorption at zero coverage, ΔG^0 , of -25 to -26 kcal/mole when Γ_s is expressed as ions/cm² (standard state = 1 ion/cm²) and q_m is between 10 and 24 $\mu\text{C}/\text{cm}^2$. The absolute value of the free energy is undoubtedly somewhat larger than this since concentrations (moles/l) were used in place of activities. These values for A and ΔG^0 compare with $A = 12$ and $\Delta G^0 = -21.6$ kcal/mole, for NCS^- ³² and $A = 6$ and $\Delta G^0 = -23$ kcal/mole for thiourea³³ at $q_m = 0$.

cis-Cr(en)₂(NCS)₂⁺. -- An analysis similar to the one above was carried out on cis-Cr(en)₂(NCS)₂⁺. $F\Gamma$ vs. potential is shown in Figure 5. Solutions more concentrated than 1.6 mM could not be studied because of the severe maxima-related problems previously mentioned. $F\Gamma$ values for 1.6 mM were arbitrarily chosen as the saturation adsorptions even though $F\Gamma$ is not yet independent of concentration at all potentials. Several lines of evidence indicate that this is not too bad an assumption. The bulkier $\text{Cr(en)}_2(\text{NCS})_2^+$ ion is expected to have $F\Gamma_s$ values less than those for $\text{Cr}(\text{NH}_3)_4(\text{NCS})_2^+$.

Figure 5. -- Adsorption of cis-Cr(en)₂(NCS)₂⁺ as a function of potential.

○ -- 1.6 mM; □ -- 0.1 mM; ◇ -- 0.033 mM;
● -- 0.01 mM; ■ -- 0.005 mM. Supporting electrolyte
0.32 M Na₂SO₄ + 0.031 M NaHSO₄.



At most potentials the $F\Gamma$ change accompanying a doubling of the solution concentration from 0.8 to 1.6 mM is very near the precision of the technique. Also, the relatively small dependence of $F\Gamma$ on potential for concentrations greater than 0.8 mM contrasts with the behavior at lower concentrations. In any case, using a saturation value somewhat less than the true value will make little difference in the trends discussed below. A similar statement can be made concerning the potential dependent Γ_s at positive potentials.

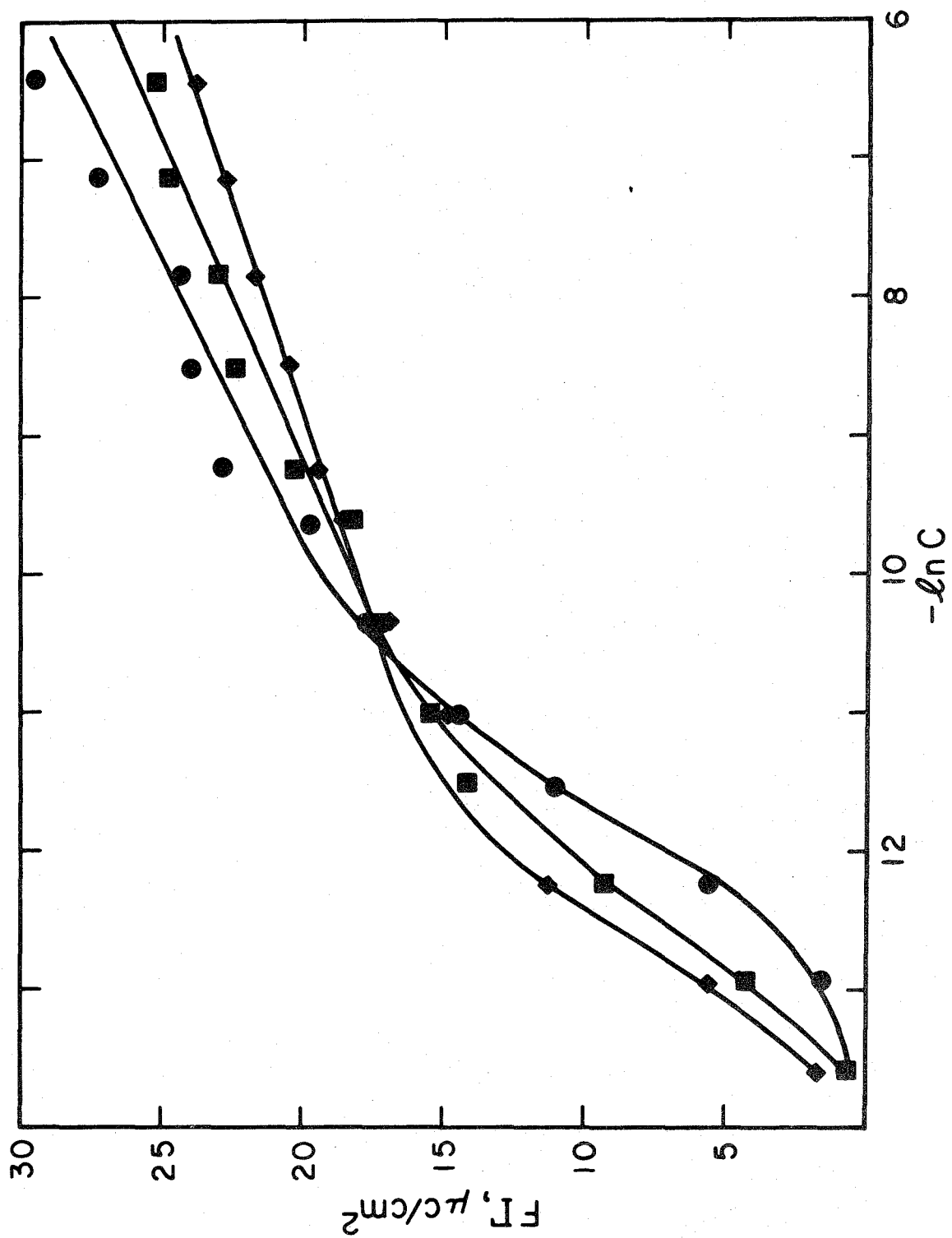
One obvious difference in the adsorptive behavior of cis- $\text{Cr(en)}_2(\text{NCS})_2^+$ and cis- $\text{Cr(NH}_3)_4(\text{NCS})_2^+$ is the decrease in adsorption of cis- $\text{Cr(en)}_2(\text{NCS})_2^+$ at lower concentrations as the potential is made more positive. This is also seen by comparing Figures 6 and 2. The data in Figure 6 is plotted at constant charge since it is generally conceded that for charged species electrode charge and not potential is the electrical variable to be controlled.³⁴ (However the general trends and curve shapes do not change if plotted at constant potential.)

The $F\Gamma$ vs. $-\ln c$ isotherms for cis- $\text{Cr(en)}_2(\text{NCS})_2^+$ and $\text{Cr(NH}_3)_4(\text{NCS})_2^+$ are not congruent (i. e., the curves at different charges or potentials cannot be superimposed by sliding the curves along either axis) for either constant charge or potential. This is somewhat surprising since most ionic systems are to at least a first approximation congruent for charge.³⁵ This lack of congruency is consistent with either a charge dependent interparticle interaction or charge dependent Γ_s or both.

Figure 6. -- Adsorption of cis-Cr(en)₂(NCS)₂⁺ as a function of $-\ln C$ (C in mole/l).

● -- $Q_m = +16$; ■ -- $Q_m = 10$, ◆ -- $Q_m = 4 \mu\text{C}/\text{cm}^2$.

Supporting electrolyte = 0.32 M Na₂SO₄ + 0.031 M NaHSO₄.



The adsorption data is replotted on Langmuirian coordinates in Figure 7. As was found for $\text{Cr}(\text{NH}_3)_4(\text{NCS})_2^+$ some attractive interactions are indicated. Curves for intermediate charges lie between the ones shown with a smooth transition being evident. The data are fitted to as Frumkin isotherm in Figure 8. Again there is considerable scatter of data in the attractive regions but fairly good fits to straight lines in the repulsive regions. The transition from predominately attractive to repulsive interactions occurs at lower coverages than for cis- $\text{Cr}(\text{NH}_3)_4(\text{NCS})_2^+$. The attractive interactions are very similar in magnitude to those for cis- $\text{Cr}(\text{NH}_3)_4(\text{NCS})_2^+$. If Γ_s were independent of q_m , a systematic increase in ΔG^0 would be indicated by the decrease in the intercept as q_m become smaller. Table III contains the least-squares slopes and intercepts for the data analyzed as in Figure 8. Because of the variation in Γ_s with q_m , ΔG^0 only varies from -25.8 to -26.2 kcal/mole in the attractive region and from -27 to -29 kcal/mole in the repulsive as q_m goes from 14 to 0 $\mu\text{C}/\text{cm}^2$. For a compound obeying a simple Frumkin isotherm, a 2 kcal variation in adsorption standard free energy as the charge is varied would be considered significant. (For $I^- \Delta G^0$ changes by 10 kcal/mole³¹ as q_m is varied from +10 to -10 $\mu\text{C}/\text{cm}^2$.) With the present complicated isotherm attaching much significance to a 2 kcal variation is highly suspect even though it is consistent with the trends in Figures 5 and 6. No trend is evident for the value of A in Table III with all values being within experimental error. The trend for B for $6 < q_m < 0$ is probably not real. At the concentrations and potentials corresponding

Figure 7. -- Adsorption of cis-Cr(en)₂(NCS)₂⁺¹ plotted on Langmuirian coordinates, $\ln \frac{\theta}{1-\theta}$ vs. $-\ln C$ (C in mole/l).
● -- $Q_m = 16 \mu\text{C}/\text{cm}^2$; ■ -- $Q_m = 10 \mu\text{C}/\text{cm}^2$.
Dashed line = Langmuir isotherm. Supporting electrolyte = 0.32 M Na₂SO₄ + 0.031 M NaHSO₄.

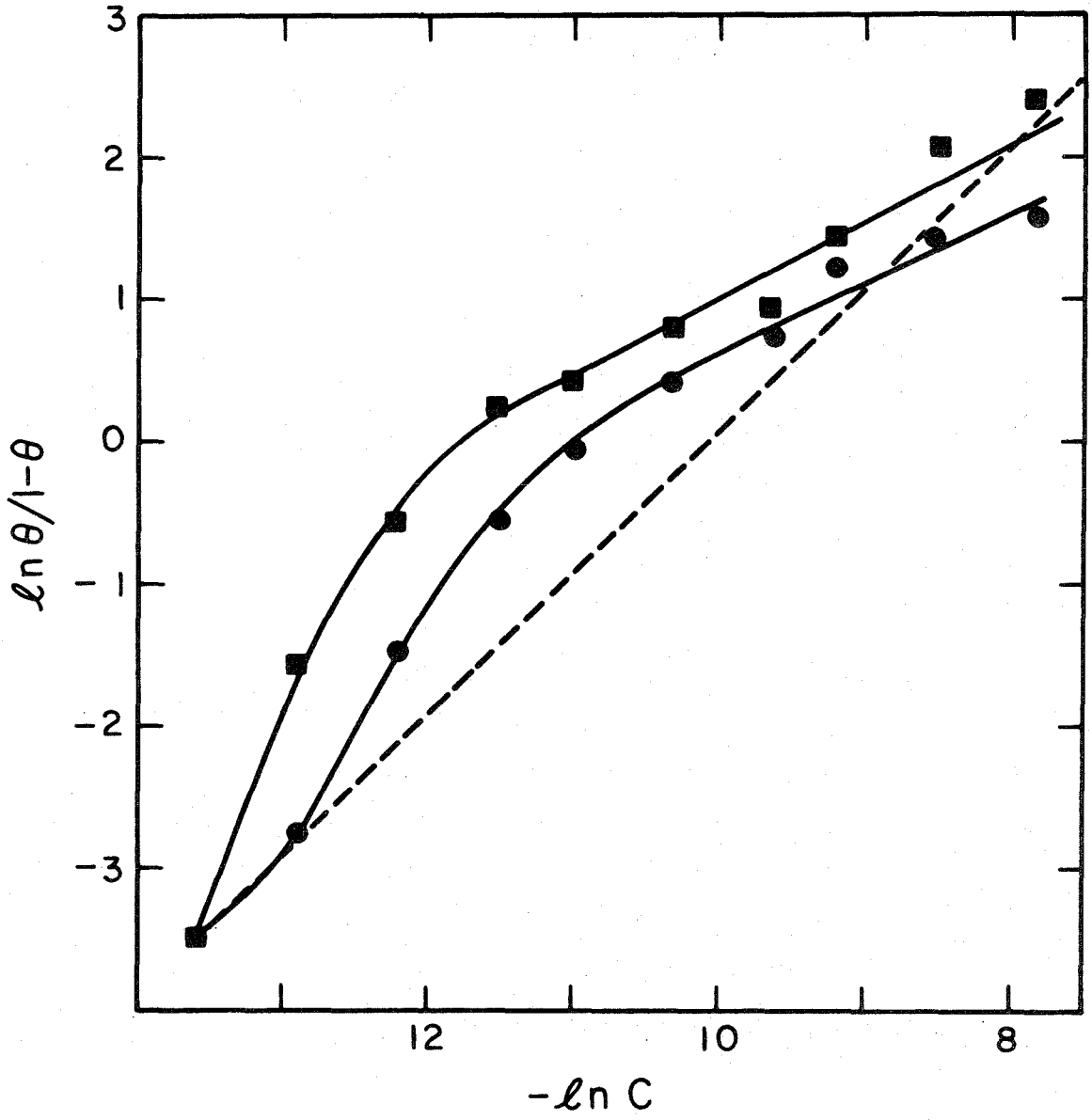


Figure 8. -- Adsorption of cis-Cr(en)₂(NCS)₂⁺ fitted to a Frumkin isotherm. Coordinates derived as in Figure 4. Solid lines are least-squares fit to descending points and dashed line fit to ascending points.

I -- $Q_m = 16 \mu\text{C}/\text{cm}^2$; $A = -2.67$, $\text{cept} = -10.07$;

II -- $Q_m = 10 \mu\text{C}/\text{cm}^2$; $A = -2.82$, $\text{cept} = -10.4$;

III -- $Q_m = 6 \mu\text{C}/\text{cm}^2$; $A = -2.63$, $\text{cept} = -10.9$.

Supporting electrolyte = 0.32 M Na₂SO₄ + 0.031 M NaHSO₄.

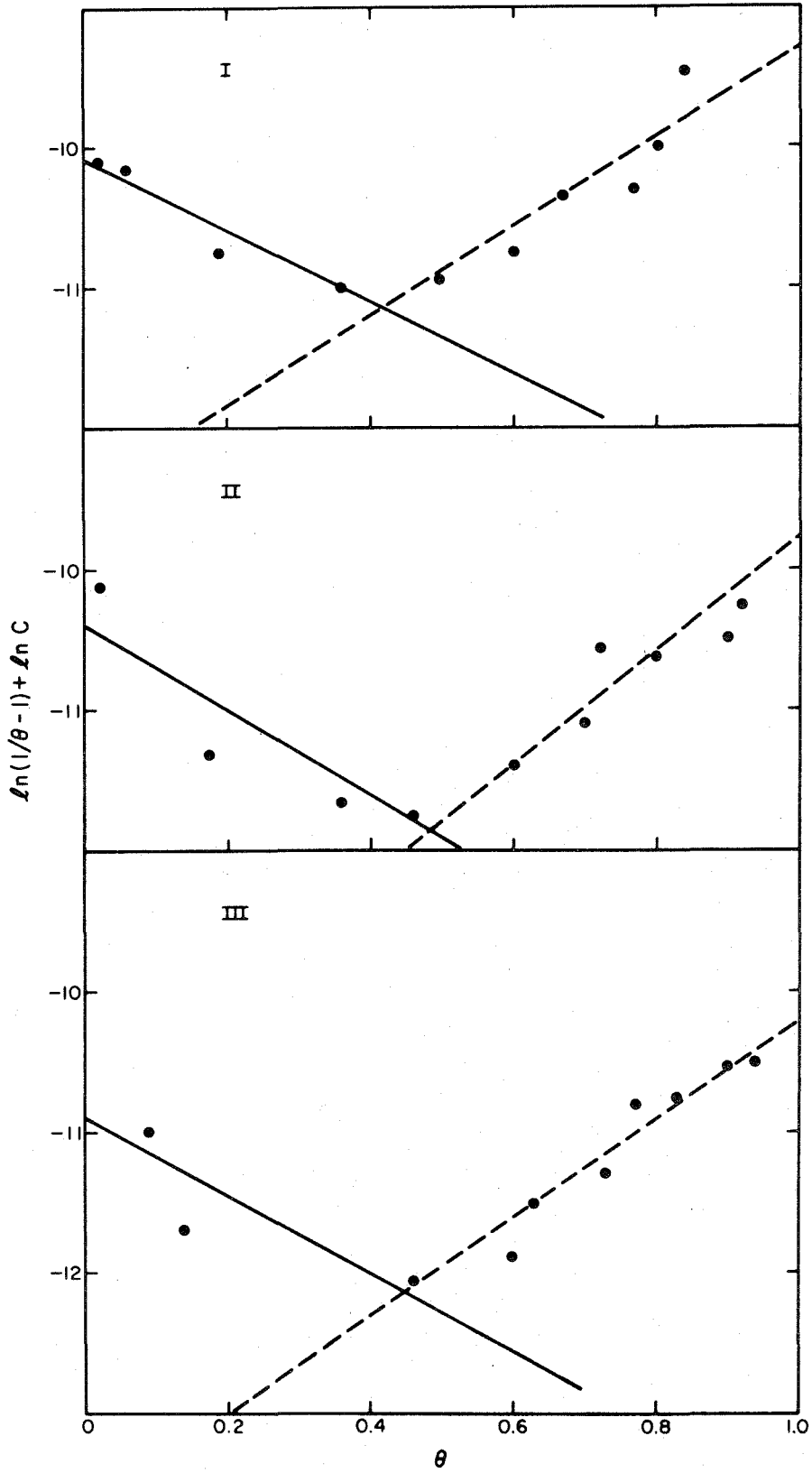


TABLE III

ADSORPTION-FREE ENERGIES AND INTERACTIONS PARAMETERS FOR

	cis-Cr(en) ₂ (NCS) ₂ ⁺ *									
Q _m (μC/cm ²)	16	14	12	10	8	6	4	2	0	
+ΔG ⁰ /RT + lnΓ _S (descending data)	-10.1	-10.2	-10.3	-10.4	-10.6	-10.9	-11.0	-11.0	-11.0	-11.0
A	-2.7	-2.8	-2.8	-3.3	-2.63	-2.37	-2.37	-2.34	-2.15	
+ΔG ⁰ /RT + lnΓ _S (ascending data)	-12.2	-13.4	-13.5	-13.5	-13.5	-13.9	-14.6	-14.6	-16.0	
B	2.8	4.0	3.6	3.5	3.2	3.7	4.8	5.0	9.2	

101

* Obtained from least-squares analysis of data, Intercept = +ΔG/RT + lnΓ_S and Slope = A or B.

to this region, the adsorption measurements were degraded by maxima at the HMDE.

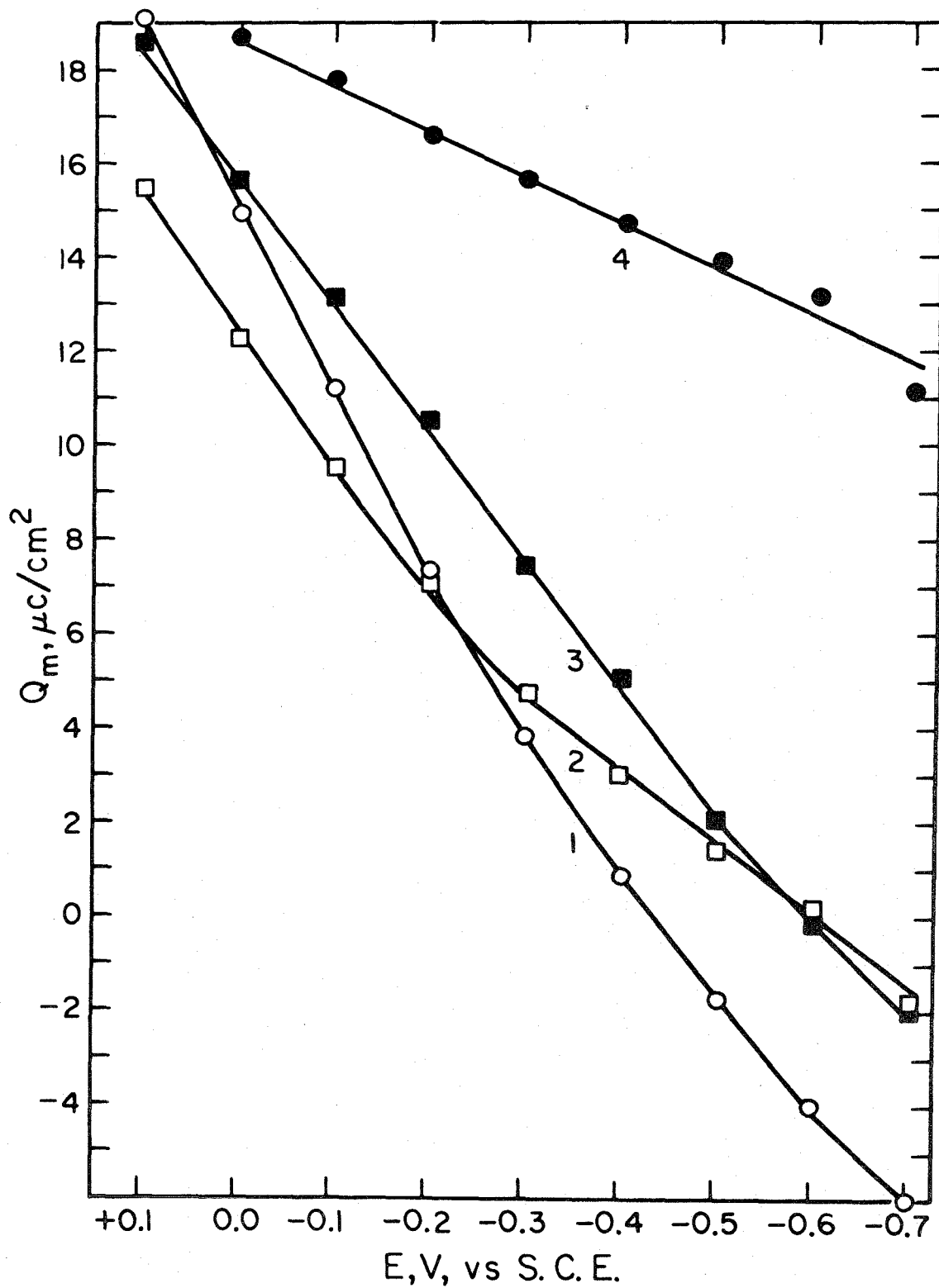
It is somewhat interesting that cis-Cr(en)₂(NCS)₂⁺ and Cr(NH₃)₄(NCS)₂⁺ shift the point of zero charge (PZC) to more negative potentials (Figure 9). It is normally found that specifically adsorbed anions shift the PZC negative while cations shift it positive. For example, the PZC in 0.01 M NaSCN³⁶ is ~ -0.55 V vs. SCE, in 8.9 × 10⁻³ M n-hexyltriethylammonium cation (+1 M KCl) ~ -0.32 V vs. SCE³⁷ and in non-specifically adsorbed NaF³⁸ ~ -0.43 V vs. SCE. In the chromium thiocyanate complexes, the thiocyanate dipole apparently dominates over the complex charge in determining the shift of the PZC.

trans-Cr(NCS)₄(NH₃)₂⁻ and Cr(NCS)₆⁻³. -- A comparison of some negatively charged thiocyanato complexes with the above positive complexes seemed desirable to see how wide spread the behavior already described might prove to be. It was in this spirit that an investigation of trans-Cr(NCS)₄(NH₃)₂⁻ and Cr(NCS)₆⁻³ was undertaken.

The results were unexpected. The chronocoulometric intercepts for both complexes increased as the concentration was lowered from 2.4 to ~0.4 mM. The slopes for trans-Cr(NCS)₄(NH₃)₂⁻ were considerably too high for all concentrations where meaningful slopes could be obtained, c ≤ 0.1 mM. Cr(NCS)₆⁻³, on the other hand, had slopes that were too low down to 0.8 mM. The standard deviations of the slopes were also quite high. These results indicate that a more complicate process than a simple diffusion controlled reaction is

Figure 9. -- Charge on metal, Q_m , as a function of the electrode potential for,

- 1 -- ○, 0.32 M Na_2SO_4 + 0.031 M NaHSO_4 ;
- 2 -- □, 1 plus 0.8 mM cis- $\text{Cr}(\text{en})_2(\text{NCS})_2^+$;
- 3 -- ■, 1 plus 0.8 mM cis- $\text{Cr}(\text{NH}_3)_4(\text{NCS})_2^+$;
- 4 -- ●, 1 plus 0.8 mM trans- $\text{Cr}(\text{NCS})_4(\text{NH}_3)_2^-$.

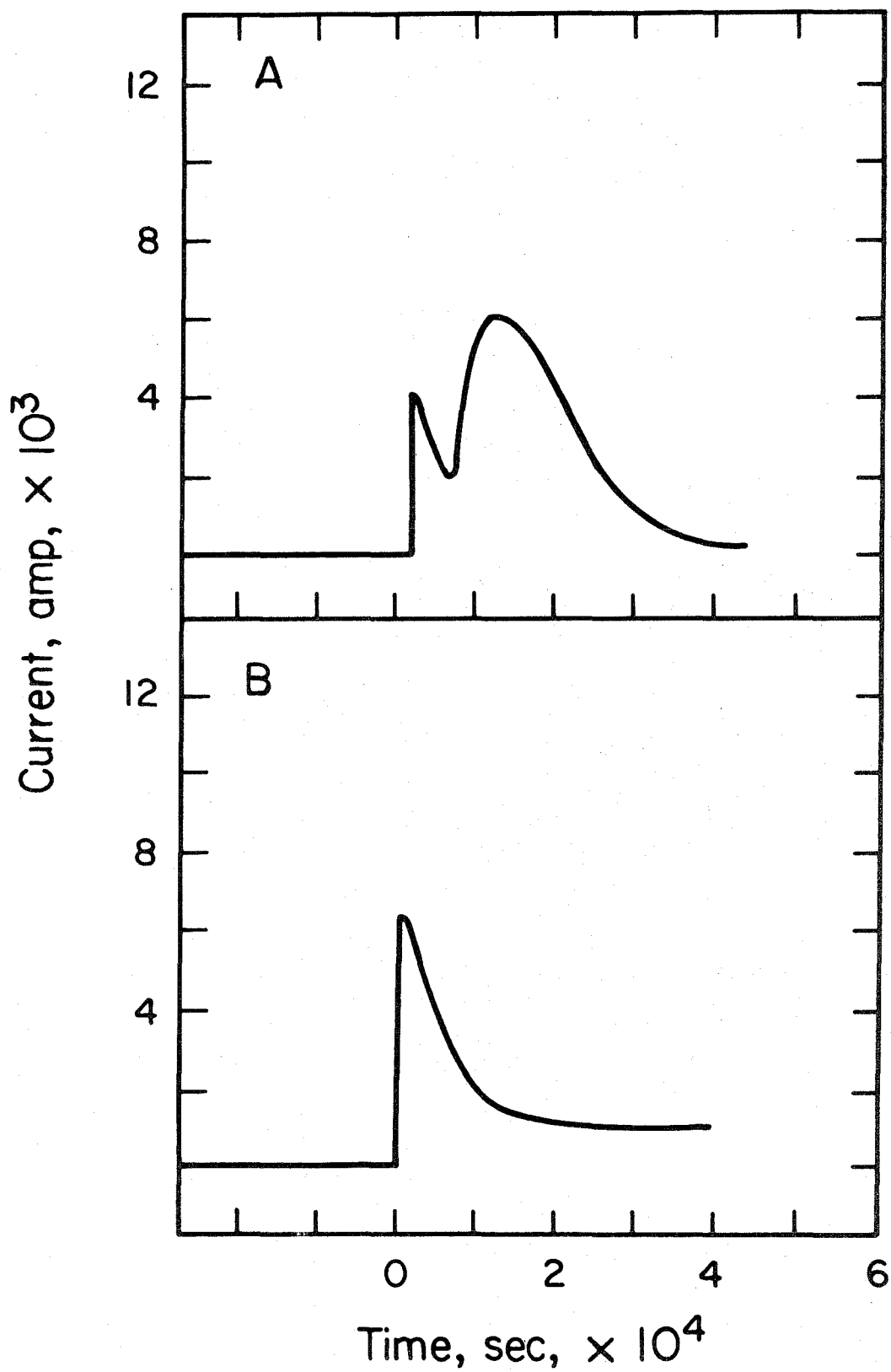


taking place. The intercepts then gradually decreased as the concentration was lowered into the micromolar region where a sudden decrease took place over an approximately four fold change in concentration. From 0.4 mM down, the behavior at least approximates that for $\text{Cr(en)}_2(\text{NCS})_2^+$ and $\text{Cr}(\text{NH}_3)_4(\text{NCS})_2^+$.

Figure 9 gives the q_m - E behavior for trans- $\text{Cr}(\text{NCS})_4(\text{NH}_3)_2^-$. The capacitance of the electrode has apparently been increased greatly by adsorption. Although the available potential range is not as large for $\text{Cr}(\text{NCS})_6^{-3}$ as for trans- $\text{Cr}(\text{NCS})_4(\text{NH}_3)_2^-$, all indications are that the former behaves similarly. At -0.3 V $q_m = 14.8 \mu\text{C}/\text{cm}^2$ and at -0.2 V $q_m = 20.1 \mu\text{C}/\text{cm}^2$ for a 0.2 mM concentration of $\text{Cr}(\text{NCS})_6^{-3}$. The shift in PZC must be enormous in both instances.

It is quite obvious from Figures 1 and 5 that $\text{Cr(en)}_2(\text{NCS})_2^+$ and $\text{Cr}(\text{NH}_3)_4(\text{NCS})_2^+$ have much smaller tendencies to be adsorbed on negatively charged surfaces (the PZC is at ~ -0.6 V) than on positive surfaces. In the present case, if the PZC is shifted negative enough, the complexes may still be strongly adsorbed at the final potential used in the chronocoulometric experiments, -1.35 V. If the adsorbed complexes were not reduced instantaneously and either physically blocked the reduction of nonadsorbed complex on the covered portions of the electrode or suppressed reduction via a ϕ_2 effect, an explanation to account for the above results might be possible. Figure 10A shows a typical i - t curve for trans- $\text{Cr}(\text{NCS})_4(\text{NH}_3)_2^-$ and 10B the behavior for cis- $\text{Cr(en)}_2(\text{NCS})_2^+$ under chronocoulometric conditions. 10B is the curve expected for an uncomplicated instantaneous reduction of an

Figure 10. -- i-t curves at a HMDE for
A -- 1.6 mM trans-Cr(NCS)₄(NH₃)₂⁻ and
B -- 0.4 mM cis-Cr(en)₂(NCS)₂⁺. Potential stepped
from 0.0 to -1.35 V (A) or -0.2 to -1.15 V (B).



adsorbed complex plus diffusion limited reduction of any complex diffusing in from bulk solution. In 10A the initial instantaneous rise and then decay of current is apparently due to reduction of adsorbed complex plus any q_m changes that take place as the coverage decreases. At the same time as the coverage decreases, the electrode becomes unblocked permitting reduction of diffusing species giving rise to another increase in current and then decay. The higher current flowing at any given time could well give rise to an increased coulometric slope. Under the same conditions as above and after a considerable decay of the initial current, the current for $\text{Cr}(\text{NCS})_6^{-3}$ is independent of concentration. For a diffusion controlled process a direct proportionality between current and concentration is expected. The electrode appears to be blocked (or reduction of unadsorbed complex suppressed), at much longer times than it is for trans- $\text{Cr}(\text{NCS})_4(\text{NH}_3)_2^-$. A resultant decrease in chronocoulometric slope might be expected.

Sufficient data are not available to give an unequivocal explanation of what is happening at the electrode surface. A non-instantaneous reduction of the adsorbed complexes seems certain. Competition between adsorption and reduction of diffusing species may also be taking place. The combined effect may be a kinetic contribution to the intercept.³⁹ At higher concentrations adsorption may be competitive enough with reduction that the electrode remains blocked for longer times than at lower concentrations. The longer the electrode is blocked the more pronounced the kinetic effect and the lower the

intercepts. A discussion of the kinetics for reduction of adsorbed complexes including at least one reaction pathway which could lead to a slower reduction for adsorbed species than diffusing ones has been given by Anson and Rodgers.⁴⁰

Chromium(III) and Cobalt(III) Azides. -- The adsorption of several azido complexes were investigated in order to compare the adsorption of analogous azide and thiocyanate complexes and to see the effect of the central metal ion on the adsorption.

$\text{Cr}(\text{NH}_3)_5\text{N}_3^{+2}$ was found not to be adsorbed up to 0.8 mM between -0.7 to +0.3 V. trans- $\text{Co}(\text{en})_2(\text{N}_3)_2^+$ was also not adsorbed. 0.8 mM cis- $\text{Cr}(\text{H}_2\text{O})_4(\text{N}_3)_2^+$ was adsorbed to less than $3 \mu\text{C}/\text{cm}^2$. The adsorption found for cis- $\text{Cr}(\text{en})_2(\text{N}_3)_2^+$ and cis- $\text{Co}(\text{en})_2(\text{N}_3)_2^+$ is tabulated in Table IV. The adsorption values for cobalt are minimum adsorptions due to the closeness of E_1 to the onset of reductive currents. The maximum discussed in connection with potential sweep and polarographic experiments prevented determination of adsorption for more concentrated solutions. For pH's less than about 4 the chronocoulometric slopes and intercepts for cis- $\text{Cr}(\text{en})_2(\text{N}_3)_2^+$ were pH dependent and increased as the pH was lowered. The reduction of adsorbed complex produces high concentrations of Cr(II) and HN_3 at the electrode surface which rapidly react to produce more Cr(III). Reduction of the catalytically produced Cr(III) at the electrode gives the appearance of more adsorption (higher intercepts) than is actually present. Between pH 4 and 7, the intercepts and slopes were independent of pH (no catalysis) if the potential was less than -0.1 V. At these pH's

TABLE IV
 ADSORPTION^a OF cis-Co(en)₂(N₃)₂⁺ AND cis-Cr(en)₂(N₃)₂⁺

E _i ^b	Co ^c			0.8 ^e	Cr ^d		
	0.8	0.4	0.2 mM		0.4 pH=2	0.2 mM pH=5	0.2 mM
0.35	14.1	11.9	6.8		13.5	14.0	
0.3	10.8	8.7	5.3		12.2	12.2	
0.2					9.3	9.3	
0.1					8.1	5.6	
0.0				7.6	7.0	4.1	2.5
-0.1				7.2	7.0	3.8	2.4
-0.2				7.6	7.5	3.8	3.0
-0.3				8.5	9.0	4.7	2.6
-0.4				8.9	9.9	5.3	2.8
-0.5				9.3	10.6	5.5	3.2
-0.6				9.7	9.9	5.3	2.9

^a Adsorption = FI in $\mu\text{C}/\text{cm}^2$, the electrolyte was 1 M NaClO₄.

^b vs. SCE.

^c pH < 2.

^d In most experiments, pH = 5.

^e Analysis of the initial data points indicate that these values are perhaps 2 $\mu\text{C}/\text{cm}^2$ too large.

the unavoidable decomposition of a small amount of complex is sufficient to drive the pH higher, often to pH higher than 7 (determined by measuring pH shortly after adding the complex to the solution). Formation of HgO at the electrode can occur positive of -0.1 V for pH's $> 6-7$. The amount formed depends on pH and can become quite large when the pH > 7 . For this reason accurate adsorption measurements were not possible positive of 0 V at these pH's. A reasonable estimate of the adsorption in this region can be made by noticing that the apparent adsorption at pH 2 is about twice the adsorption measured at pH 5 (because of catalysis) for potentials negative of -0.1 V where the intercepts are pH independent (pH > 4). Since there should be no contribution to the intercept from HgO reduction at pH 2, dividing the pH 2 results in Table IV by 2 and using these values as a measure of the adsorption at positive potentials is reasonable.

Table IV and the discussion present above would indicate that the cobalt complex is adsorbed to about twice the extent as the chromium complex at $+0.35$ V.

Complete adsorption isotherms are necessary before a definitive statement concerning the significance of these results can be made. These isotherms, unfortunately, are not available to us. However, the evidence is still strong that the cobalt, with a higher LFSE, is intrinsically more strongly adsorbed than the chromium. cis-Cr(en)₂(N)₃⁺ is definitely adsorbed to a greater extent than cis-Cr(H₂O)₄(N₃)₂⁺.

Some adsorption measurements were also made in sulfate electrolyte. Adsorption of 0.8 mM cis-Co(en)₂(N₃)₂⁺ was decreased to ~3 μC/cm² at +0.35 V. Adsorption of cis-Cr(en)₂(N₃)₂⁺ was not affected for potentials less than -0.2 V but decreased rapidly for potentials positive of this. SO₄⁻² would seem to be more strongly adsorbed than ClO₄⁻ at positive potentials and to be desorbing the complexes.

DISCUSSION

By far, the most remarkable aspect of the adsorption of the transition-metal azide and thiocyanate complexes on mercury electrodes is its strength. In most cases the complexes are adsorbed much more strongly than free azide and thiocyanate ions themselves. In terms of surface activity the difference in adsorbabilities is even greater. The electrode surface is virtually saturated in 1 mM solutions of cis-Cr(NH₃)₄(NCS)₂⁺ and cis-Cr(en)₂(NCS)₂⁺ while even in 1 M NCS⁻ the surface is less than half covered.³³ This unusually strong adsorption, some of the peculiar aspects of the adsorption isotherms, and the strong dependence of the adsorption on the coordinated ligands other than thiocyanate and azide indicate that these transition-metal complexes represent a new and unique class of adsorbable compounds.

The nature of the forces resulting in the specific adsorption of simple monatomic ions is still not fully understood and retains controversial aspects. Grahame⁴¹ originally introduced the idea of covalent bond formation between the specifically adsorbed ions and the electrode. Covalent bond formation, however, has been refuted by several workers.^{42, 43, 44} Bockris et al.^{43, 44} considered the possible factors affecting specific adsorption of ions and were able to calculate reasonable standard free energies of adsorption assuming no bond formation with the electrode. Bockris concluded that solvation energies were the primary forces dictating adsorption. Bockris'

work is open to criticism on several grounds. The calculated image and dispersion forces are considerably greater than what is usually encountered.⁴⁵ Also, it is difficult to understand the strong adsorption of NCS^- and $(\text{NH}_2)_2\text{CS}$ and the much weaker adsorption of NCO^- and $(\text{NH}_2)_2\text{CO}$ ³³ without invoking bond formation. Barclay⁴⁶ has suggested that specific adsorption is essentially a hard and soft interaction between the ion and the electrode and, therefore, encompasses both ionic and covalent forces. It seems reasonable to assume that all of these factors may be important to a more or lesser degree and should be included in any discussion concerning the strength of specific adsorption.

The primary driving force for adsorption of the complexes is undoubtedly the same as that for the free ligands, namely bond formation between the sulfur of thiocyanate and the nitrogen of azide and the electrode. The stronger adsorption of the thiocyanate complexes over that for the azides is simply a reflection of the greater tendency for free thiocyanate to adsorb than azide.⁴⁷ The assumed similarity between the adsorptive driving forces for the complexes and the free ligands also allows a relatively simple interpretation of the eventual desorption of the strongly adsorbed thiocyanate complexes at negative potentials. The standard free energy of adsorption can be considered to consist of a field independent term plus the sum of a power series in the electrical field, X , in the inner region of the double layer,⁴⁸ i. e.,

$$\Delta G^0/RT = \Delta G^{0'}/RT + aX + bX^2 + cX^3 + \dots$$

The term aX can be considered to arise from the interaction of the charge on the ion or permanent dipole with the field. In the case of thiocyanate, ΔG^0 is expected to increase as the field (or electrode charge) is made less positive and a resulting decrease in adsorption found. Such is the behavior observed experimentally.³² With the metal complexes the situation is somewhat more complicated since the interaction of the field with charge on the metal is opposite that of the coordinated thiocyanates. However, the center of charge on the metal ion lies in a lower field region than the thiocyanate and it is therefore not unreasonable that the adsorption decrease as q_m decreases.

Coordination of NCS^- to the electropositive chromium(III) would be expected to decrease the strength of the sulfur-mercury bond involved in the adsorption of NCS^- at the electrode (in much the same way that the bond between sulfur and mercury(II) is weakened in $CrNCSHg^{4+2}$). A comparison of the results in Table II with the previous results for NCS^- ⁴⁹ under similar conditions suggest that such might be the case. The results are not strictly comparable since the absolute charge on some of the chromium complexes is greater than for NCS^- . However, the much larger size of the chromium complex would tend to minimize any solvation differences. The role that solvation might play is demonstrated by noting that $Cr(NH_3)_5NCS^{+2}$ is less strongly adsorbed than trans- $Cr(en)_2(NCS)_2^+$ (Table II).

On the other hand, it might be interesting to speculate that the difference in the adsorption between these two complexes results

because trans-Cr(en)₂(NCS)₂⁺ binds to the electrode with both thiocyanates. If the complex positions itself on the electrode such that the plane of ethylenediamine ligands is perpendicular instead of parallel to the electrode surface with no two nitrogen atoms of a single ethylenediamine molecule next to the electrode, it might be possible for such a mode of adsorption to take place, if double bonds connect nitrogen to carbon and carbon to sulfur in the thiocyanate ligands. With this bonding scheme the NCS ligands are not perpendicular to the plane of the ethylenediamine ligands and can slant toward the electrode. Under certain conditions, this bonding scheme prevails in Reinecke salt instead of N≡C-S⁻.²⁹

The multiple bond formation with the electrode that is possible with the cis-azido and thiocyanato complexes is most certainly the reason that these compounds are so strongly adsorbed. The formation of two bonds more than compensates for any decrease in bond strength resulting from coordination of thiocyanate and azide to a metal ion. Also, to be considered in this regard is the very favorable entropy gain of having two adsorbable entities coordinated to single central metal.

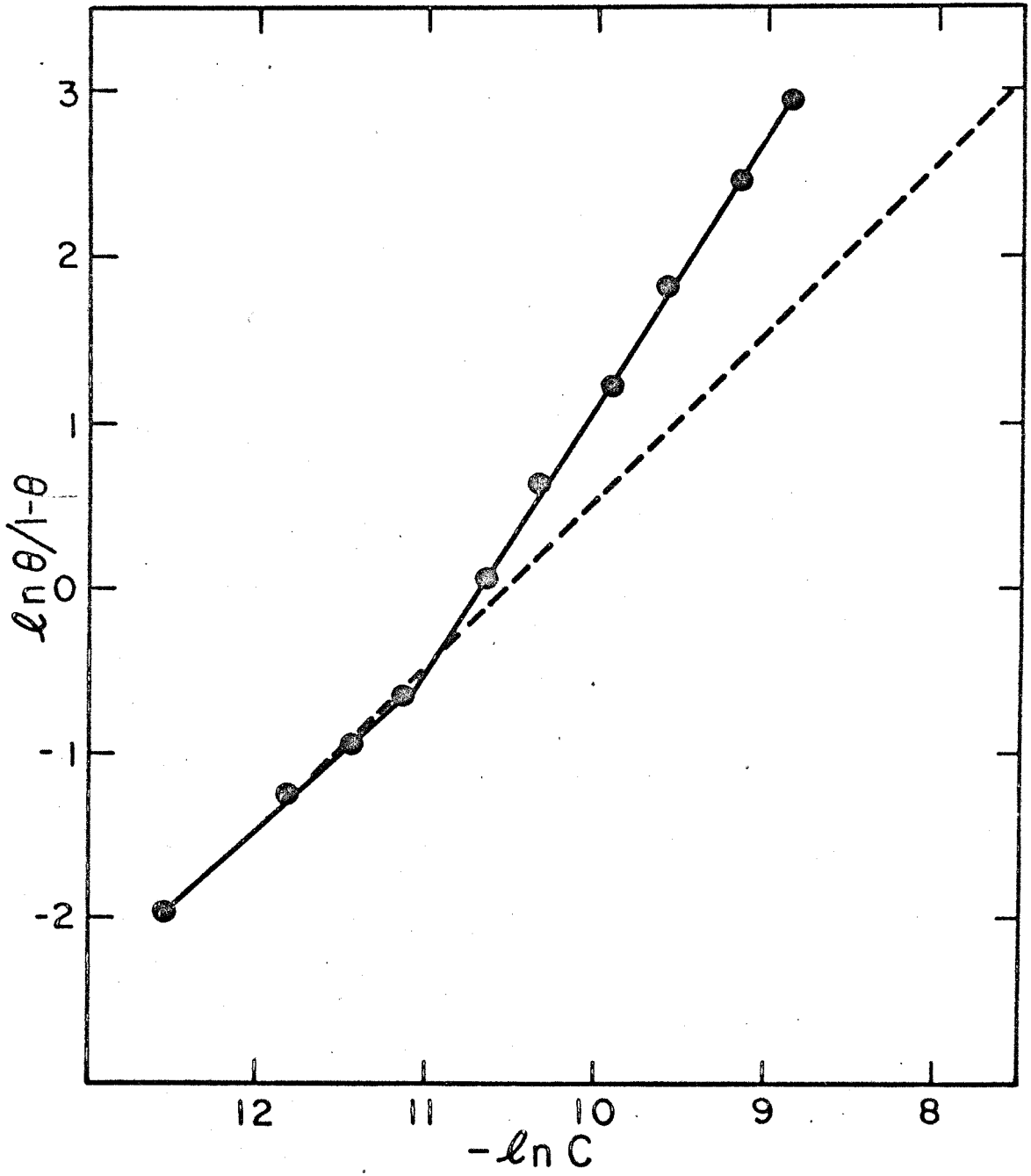
The Interaction Parameters A and B. -- A change from predominantly attractive to repulsive interactions (the A term in eqn. (1)) is not an entirely unknown phenomenon.⁵⁰ The change from attractive to repulsive interactions though, usually results from a change in orientation of the adsorbed species brought about a change in electrode potential or charge. However, the thiocyanate complexes appear

to represent the only known compounds to have such a dramatic reversal in the value of the interaction parameter without changing the charge (or potential) of the electrode.

The repulsive interactions at high coverages ($\theta > 0.5$ or 0.8) are easy enough to understand because they correspond to the familiar repulsive dipole-dipole and ion-ion interactions observed at all coverages for most species that obey the Frumkin isotherm. Fairly strong repulsive forces might be expected to result from interactions between both the positively charged metal centers on the surface and the sulfur atoms of the adsorbed thiocyanate ligands. Unless they, yet to be explained, attractive forces are quite strong the repulsive forces should dominate at high coverages since for $\theta > 0.5$ the separation between adsorbed molecules is less than 1.4 times the separation on a saturated surface.⁵¹ That the change from attractive to repulsive forces occurs at lower coverages for cis-Cr(en)₂(NCS)₂⁺ than for cis-Cr(NH₃)₄(NCS)₂⁺ can be understood in terms of the interaction of the bulky coordinated ethylenediamines of adjacent molecules.

Intuition would not predict attractive interactions for the compounds under consideration. However, attractive forces appear to be the rule and not the exception for the thiocyanate complexes. Previous work with fac-Cr(H₂O)₃(NCS)₃⁴⁰ where repulsive forces should be less important showed that a definite region of coverage exists where attractive forces predominate (Figure 11). The attractive interaction parameter, *A*, was found to be -2.4, very similar to the parameters for cis-Cr(en)₂(NCS)₂⁺ and Cr(NH₃)₄(NCS)₂⁺.

Figure 11. -- Adsorption of $\text{fac-Cr(H}_2\text{O)}_3(\text{NCS})_3$ plotted on Langmuirian coordinates, $\ln \frac{\theta}{1-\theta}$ vs. $-\ln C$ (C in mole/l). Dashed line = Langmuir isotherm. Supporting electrolyte, 1 M NaClO_4 , pH < 2.



In this respect it might also be mentioned that there is circumstantial evidence that the negatively charged trans-Cr(NCS)₄(NH₃)₂⁻ and Cr(NCS)₃⁻³ behave similarly. The sudden decrease in the chronocoulometric intercepts as the concentrations are decreased is most easily understood as being due to attractive forces between adsorbed molecules in a similar fashion to the sudden decreases for cis-Cr(en)₂(NCS)₂⁺ and cis-Cr(NH₃)₄(NCS)₂⁺ (Figures 2 and 6).

For the charged species, the attractive interactions at lower coverages could be rationalized as being due to the attractive forces between the positively charged chromium and the negatively charged adsorbed sulfate. Were this to be true a very large potential or charge dependence would be expected in the value of A. No such dependence of A on charge (or potential) was observed. The net zero charge of fac-Cr(H₂O)₃(NCS)₃ precludes interactions of this type with adsorbed electrolyte. Alternatively one might suggest an isotherm that takes into account possible competitive adsorption of both SO₄⁻² and the metal complex should have been used. The Frumkin isotherm in this situation becomes⁵²

$$\beta c = \theta_1 / (1 - \theta_1 - \theta_2) \exp A \theta_1 \quad (3)$$

where θ_1 is the coverage by chromium and θ_2 the coverage by SO₄⁻² or ClO₄⁻. An isotherm such as (3) could not explain the results for either fac-Cr(H₂O)₃(NCS)₃ or cis-Cr(en)₂(NCS)₂⁺ because attractive interactions for fac-Cr(H₂O)₃(NCS)₃ occur at coverages of the complex where electrolyte adsorption should be small ($\theta_2 \ll 1$) and similarly

for cis-Cr(en)₂(NCS)₂⁺ with attractive interactions being present at charges not conducive to SO₄⁻² adsorption. Competitive adsorption, though, seems a reasonable explanation for the decrease in adsorption at constant concentration for Cr(en)₂(NCS)₂⁺ positive of -0.2 V. Strong sulfate adsorption may hinder the adsorption of cis-Cr(en)₂(NCS)₂⁺ in this region.

Yet another alternative is an induced heterogeneity mechanism similar to that proposed previously.^{51, 53} Binding of the sulfur with the electrode may result in some polarization of the 6s electrons in the mercury toward the electropositive chromium. This polarization would necessarily favor adsorption of the complex but it would not come close to compensating for the unfavorable interaction of the 6s electrons of the mercury with the bonding electrons of the sulfur. It would, however, decrease the net electron density in the remaining 6s orbitals. A weaker antibonding interaction between the electron pair of the sulfur atom and the 6s electrons of mercury atoms in the electrode would result. It might then be easier for each successive molecule to adsorb giving rise to apparent attractive forces.

The deviations of the data were large enough that we were unable to determine the powers of θ in eqn. (2). There are a number of interactions that give rise to various powers of θ ^{43, 51} and if all these forces are active, it is quite possible that no single power of θ will suffice even over a small range of θ .

The LFSE Correlation. -- The apparent correlation between LFSE and the amount of adsorption has intrigued us for quite some-time. In every case where a correlation was possible the adsorption was higher for the compound with the highest LFSE. Since many of the compounds in the previous studies were labile, however, the correlation between LFSE and adsorption is somewhat tenuous because the concentrations and identities of the constituents in the solutions were not always known. The compounds in the present study are substitutionally inert and the concentration and identity of the adsorbing species is known with certainty. cis-Co(en)₂(N₃)₂⁺ with 24 Dq of LFSE is more strongly adsorbed than cis-Cr(en)₂(N₃)₂⁺ with 12 Dq (Table IV). Likewise, the adsorptions of cis-Cr(en)₂(N₃)₂⁺ compared to cis-Cr(H₂O)₄(N₃)₂⁺, and cis-Cr(en)₂(NCS)₂⁺ and cis-Cr(NH₃)₄(NCS)₂⁺ compared to cis-Cr(H₂O)₄(NCS)₂⁺ (Table V) correlate well with their LFSE's.

It has been previously noted^{1, 2} that when Cr(H₂O)₅NCS⁺² reacts with Hg⁺² in homogeneous solution there is an increase in the LFSE. If a similar increase in LFSE was to obtain when the coordinated thiocyanate binds with the mercury electrode, this increase would represent an additional driving force for the adsorption. In order for there to be a correlation between adsorption for a given central metal ion, but with different ligands, and LFSE, the increase in LFSE would itself have to be dependent on the original LFSE. One would not guess this to be the case before hand but in practice this is what is observed. Table VI lists several chromium thiocyanates and

TABLE V

ADSORPTION^a of cis-Cr(H₂O)₄(NCS)₂⁺, cis-Cr(en)₂(NCS)₂⁺ AND cis-Cr(NH₃)₄(NCS)₂⁺

E (mV vs. S. C. E.)	Cr(H ₂ O) ₄ (NCS) ₂ ⁺ , ^{b, c}	Cr(en) ₂ (NCS) ₂ ⁺ , ^b	Cr(NH ₃) ₂ (NCS) ₂ ⁺ , ^b
200	12.5		32.4
100	10.6	25.1	32.3
0	9.8	24.4	30.4
-100	9.0	23.2	29.2
-200	7.9	22.9	27.1
-300	7.6	22.1	24.2

^a Adsorption in $\mu\text{C}/\text{cm}^2$.

^b Concentration of complexes = 0.5 mM.

^c Values from reference 7.

TABLE VI
 CHANGE IN λ_{\max} AND LFSE ON REACTING
 CHROMIUM THIOCYANATES WITH Hg^{+2}

	λ_{\max}^a ($m\mu$)	$\lambda_{\max}'^b$ ($m\mu$)	ΔLFSE^c (kcal/mole)
$\text{Cr}(\text{H}_2\text{O})_5\text{NCS}^{+2}$	565	560	0.5
$\text{Cr}(\text{NH}_3)_5\text{NCS}^{+2}$	484	469	1.9
<u>cis</u> - $\text{Cr}(\text{NH}_3)_4(\text{NCS})_2^+$	494	474	2.4

^a No Hg^{+2} present in solution.

^b Hg^{+2} present $\sim 10:1$ excess.

^c $\Delta\text{LFSE} = \left(\frac{1}{\lambda_{\max}'} - \frac{1}{\lambda_{\max}} \right) 2.86 \text{ cal cm/mole.}$

the LFSE increase resulting when the complexes are reacted with Hg^{+2} . If the complexes were to behave similarly on binding with electrode instead of Hg^{+2} , the correlation between LFSE and adsorption at least for the thiocyanates is easily explainable.

Hg^{+2} also reacts with cis-azides to form stable complexes.⁵⁴

The interaction is sufficiently weak that a noticeable change in λ_{\max} is not observed. Any ΔLFSE is likely to be smaller than for the thiocyanates. The smaller increase in LFSE might explain why $\text{Co}(\text{en})_2(\text{N}_3)_2^+$ with an enormous 24 Dq of LFSE is only somewhat more strongly adsorbed than $\text{Cr}(\text{en})_2(\text{N}_3)_2^+$ with only 12 Dq.

REFERENCES

1. D. J. Barclay and F. C. Anson, J. Electroanal. Chem., 28, 71 (1970).
2. J. N. Armor and A. Haim, J. Amer. Chem. Soc., 93, 867 (1971).
3. J. H. Espenson and W. R. Bushey, Inorg. Chem., 10, 2457 (1971).
4. S. N. Frank and F. C. Anson, ibid., 11, 2938 (1972).
5. N. Tanaka, E. Kyuno, G. Sato and R. Tamamushi, J. Phys. Chem., 66, 2703 (1962).
6. F. C. Anson and Josip Caja, J. Electrochem. Soc., 117, 306 (1970).
7. D. J. Barclay, E. Passeron and F. C. Anson, Inorg. Chem., 9, 1024 (1970).
8. E. Zinato, R. D. Lindholm, and A. W. Adamson, J. Amer. Chem. Soc., 91, 1076 (1969).
9. M. Mori, Inorg. Syn., 5, 132 (1957).
10. E. Kyuno, M. Kamada and N. Tanaka, Bull. Chem. Soc. Japan, 40, 1848 (1967).
11. P. Pfeiffer and M. Tilgner, Z. Anorgan. Chem., 55, 365 (1907).
12. P. Pfeiffer, Ber., 37, 4268 (1904).
13. C. L. Rollinson and J. C. Bailar, Jr., Inorg. Syn., 2, 200 (1946).
14. P. J. Staples and M. L. Tobe, J. Chem. Soc., 4812 (1960).
15. J. C. Bailar, Jr., Inorg. Syn., 2, 222 (1946).

16. M. Linhard and M. Weigel, Z. Anorgan. Chem., 271, 130 (1953).
17. M. Linhard and W. Berthold, ibid., 279, 173 (1955).
18. R. Snellgrove and E. L. King, J. Amer. Chem. Soc., 84, 4610 (1952).
19. A. Haim, ibid., 88, 2324 (1966).
20. G. W. Haupt, J. Res. Nat. Bur. Stand., 48, 414 (1952).
21. C. S. Garner and D. A. House, in Transition Metal Chem., Vol. 6, ed., R. L. Carlin, Marcell Dekker, New York, N. Y., 1970.
22. J. J. Lingane, "Electroanalytical Chemistry", Interscience Publishers, Inc., New York, N. Y., 1958, Chapter 19.
23. J. H. Christie, R. A. Osteryoung, and F. C. Anson, J. Electroanal. Chem., 13, 236 (1967).
24. G. Lauer and R. A. Osteryoung, Anal. Chem., 39, 1866 (1967).
25. N. Tanaka, T. Ito, and R. Tamamushi, Bull. Chem. Soc. Japan, 37, 1430 (1964).
26. E. Fischerová and O. Fischer, Coll. Czech. Chem. Commun., 26, 2570 (1961).
27. W. C. Kaska, C. Sutton, and E. Serros, Chem. Commun., 100 (1970).
28. R. G. Linck, Inorg. Chem., 11, 61 (1972).
29. Y. Takeuchi and Y. Saito, Bull. Chem. Soc. Japan, 30, 319 (1951).
30. R. A. Osteryoung and J. H. Christie, J. Phys. Chem., 71, 1348 (1967).

31. P. Delahay, "Double Layer and Electrode Kinetics", Interscience Publishers, New York, N. Y., 1965, Chapter 5.
32. S. Minc and J. Andrzejczak, J. Electroanal. Chem., 17, 101 (1968).
33. R. Parsons and P. C. Symons, Trans. Faraday Soc., 64, 1077 (1968).
34. R. Parsons, ibid., 51, 1518 (1955).
35. R. Payne, J. Electroanal. Chem., 41, 277 (1973).
36. H. Wroblowa, Z. Kovac, and J. O'M. Bockris, Trans. Faraday Soc., 61, 1523 (1965).
37. R. J. Meakins, M. G. Stevens, and R. J. Hunter, J. Phys. Chem., 73, 112 (1969).
38. C. D. Russell, J. Electroanal. Chem., 6, 486 (1963).
39. J. H. Christie, G. Lauer, and R. A. Osteryoung, ibid., 7, 60 (1964).
40. F. C. Anson and R. Rodgers, J. Electroanal. Chem., in press.
41. D. C. Grahame, M. A. Path, and J. I. Cummings, J. Amer. Chem. Soc., 74, 4422 (1952).
42. S. Levine, G. M. Bell, and D. Calvert, Can. J. Chem., 40, 518 (1962).
43. J. O'M. Bockris, M. A. V. Devanathan, and K. Müller, Roy. Soc. London, 374, 55 (1963).
44. T. N. Anderson and J. O'M. Bockris, Electrochim. Acta, 9, 347 (1964).

45. D. M. Young and A. D. Crowell, *Physical Adsorption of Gases*, Butterworth & Co. Ltd., London, 1962, Chapter 2.
46. D. J. Barclay, *J. Electroanal. Chem.*, 19, 318 (1968).
47. C. V. D'Alkaine, E. R. Gonzalez, and R. Parsons, *ibid.*, 32, 57 (1971).
48. R. Parsons, *ibid.*, 5, 397 (1963).
49. F. C. Anson and D. A. Payne, *ibid.*, 13, 35 (1967).
50. B. B. Damaskin, *Electrochim. Acta*, 9, 231 (1964).
51. E. Gileadi and B. E. Conway, *Modern Aspects of Electrochemistry*, No. 3, J. O'M. Bockris and B. E. Conway, ed., Butterworths & Co. Ltd., London, 1964, pp. 376-381.
52. Reference 45, Chapter 11.
53. M. Boudart, *J. Amer. Chem. Soc.*, 74, 1531, 3556 (1952).
54. D. A. Loeliger and H. Taube, *Inorg. Chem.*, 5, 1376 (1966).